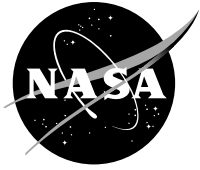


NASA/TM—2010-216772



# Fission Surface Power System Initial Concept Definition

*Fission Surface Power Team  
National Aeronautics and Space Administration  
and Department of Energy*

---

August 2010

## NASA STI Program . . . in Profile

Since its founding, NASA has been dedicated to the advancement of aeronautics and space science. The NASA Scientific and Technical Information (STI) program plays a key part in helping NASA maintain this important role.

The NASA STI Program operates under the auspices of the Agency Chief Information Officer. It collects, organizes, provides for archiving, and disseminates NASA's STI. The NASA STI program provides access to the NASA Aeronautics and Space Database and its public interface, the NASA Technical Reports Server, thus providing one of the largest collections of aeronautical and space science STI in the world. Results are published in both non-NASA channels and by NASA in the NASA STI Report Series, which includes the following report types:

- **TECHNICAL PUBLICATION.** Reports of completed research or a major significant phase of research that present the results of NASA programs and include extensive data or theoretical analysis. Includes compilations of significant scientific and technical data and information deemed to be of continuing reference value. NASA counterpart of peer-reviewed formal professional papers but has less stringent limitations on manuscript length and extent of graphic presentations.
- **TECHNICAL MEMORANDUM.** Scientific and technical findings that are preliminary or of specialized interest, e.g., quick release reports, working papers, and bibliographies that contain minimal annotation. Does not contain extensive analysis.
- **CONTRACTOR REPORT.** Scientific and technical findings by NASA-sponsored contractors and grantees.

- **CONFERENCE PUBLICATION.** Collected papers from scientific and technical conferences, symposia, seminars, or other meetings sponsored or cosponsored by NASA.
- **SPECIAL PUBLICATION.** Scientific, technical, or historical information from NASA programs, projects, and missions, often concerned with subjects having substantial public interest.
- **TECHNICAL TRANSLATION.** English-language translations of foreign scientific and technical material pertinent to NASA's mission.

Specialized services also include creating custom thesauri, building customized databases, organizing and publishing research results.

For more information about the NASA STI program, see the following:

- Access the NASA STI program home page at <http://www.sti.nasa.gov>
- E-mail your question via the Internet to [help@sti.nasa.gov](mailto:help@sti.nasa.gov)
- Fax your question to the NASA STI Help Desk at 443-757-5803
- Telephone the NASA STI Help Desk at 443-757-5802
- Write to:  
NASA Center for AeroSpace Information (CASI)  
7115 Standard Drive  
Hanover, MD 21076-1320

NASA/TM—2010-216772



# Fission Surface Power System Initial Concept Definition

*Fission Surface Power Team  
National Aeronautics and Space Administration  
and Department of Energy*

National Aeronautics and  
Space Administration

Glenn Research Center  
Cleveland, Ohio 44135

---

August 2010

## Acknowledgments

This document was written predominantly by Lee Mason from the National Aeronautics and Space Administration Glenn Research Center (GRC) and Dave Poston from Los Alamos National Laboratory (LANL) with much editing help provided by the Fission Surface Power (FSP) team. Don Palac from GRC is the FSP project manager and Lee Mason serves as the FSP principal investigator. John Warren is the NASA Headquarters program executive and Scott Harlow is the Department of Energy (DOE) program manager. The principal technical leads at the participating organizations are Mike Houts/Marshall Space Flight Center (MSFC), Jim Werner/Idaho National Laboratory (INL), Dave Poston/LANL, Lou Qualls/Oak Ridge National Laboratory (ORNL), and Ross Radel/Sandia National Laboratory (SNL). Harold Adkins from Pacific Northwest National Laboratory (PNNL) provides key design support for the NaK pumps. Abe Weitzberg and Sterling Bailey are experienced nuclear consultants that regularly contribute to the FSP team. The FSP project is part of the Exploration Technology Development Program (ETDP) managed by Frank Peri from Langley Research Center (LaRC). Diane Hope from LaRC serves as the FSP program element manager. The FSP project also has participation from industry and academia including Sunpower, Foster Miller, Barber-Nichols, Material Innovations, Advanced Cooling Technologies, Auburn, Texas A&M, University of Florida, and the Center for Space Nuclear Research at INL.

This report contains preliminary findings,  
subject to revision as analysis proceeds.

Trade names and trademarks are used in this report for identification  
only. Their usage does not constitute an official endorsement,  
either expressed or implied, by the National Aeronautics and  
Space Administration.

*Level of Review:* This material has been technically reviewed by technical management.

Available from

NASA Center for Aerospace Information  
7115 Standard Drive  
Hanover, MD 21076-1320

National Technical Information Service  
5301 Shawnee Road  
Alexandria, VA 22312

Available electronically at <http://gltrs.grc.nasa.gov>

# Contents

Executive Summary .....	1
1.0 Purpose .....	1
1.1 Affordable Fission Surface Power System Study .....	2
1.2 Preliminary Reference Concept Selection .....	2
2.0 Lunar and Mars Architecture Studies .....	3
2.1 Lunar Architecture Team .....	3
2.2 Mars Architecture Team .....	3
2.3 Lunar Surface Systems .....	4
3.0 FSP System Overview .....	7
3.1 Derived Requirements .....	7
3.2 Design Summary .....	9
4.0 Reactor Module .....	11
4.1 Key Nuclear Design Decisions .....	13
4.1.1 Nuclear Fuel Selection .....	13
4.1.2 Structural Material Selection .....	13
4.1.3 Reactor Coolant Selection .....	14
4.1.4 Radial Reflector Material Selection .....	14
4.1.5 Reactivity Control Mechanism Selection .....	15
4.1.6 Pump Technology .....	15
4.2 Core and Reflector .....	16
4.2.1 Fuel Pins .....	18
4.2.2 Core Geometry .....	18
4.2.3 Vessel and Plenum Geometry .....	19
4.2.4 Radial Reflector and Control Drums .....	19
4.3 Heat Transport .....	19
4.3.1 Number of Loops .....	20
4.3.2 System Flow Configuration .....	20
4.3.3 NaK Pumps .....	21
4.3.4 Volume Accumulators .....	22
4.3.5 Heat Exchangers .....	23
4.3.6 Other Components .....	23
4.4 Instrumentation and Control .....	24
4.5 Radiation Shield .....	26
4.6 Reactor Thermal Control .....	27
5.0 Balance-of-Plant (BOP) .....	29
5.1 Key Balance-of-Plant Design Decisions .....	29
5.1.1 Power Conversion Technology .....	29
5.1.2 Convertor Size and Number .....	30
5.1.3 Power Conversion Heat Input .....	31
5.1.4 Power Transmission .....	31
5.1.5 Power Conversion Cooling .....	32
5.1.6 Radiator Technology .....	33
5.2 Power Conversion .....	34
5.2.1 Stirling Convertor .....	34
5.2.2 Hot-Side Heat Exchanger .....	35
5.3 Heat Rejection .....	36
5.3.1 Heat Transport .....	36
5.3.2 Radiator Assembly .....	37
5.3.3 Deployment System .....	39

5.4	Power Management and Distribution .....	40
5.4.1	Local Power Controller .....	40
5.4.2	Electric Load Interface .....	41
5.4.3	Transmission Cabling .....	41
5.4.4	Solar Array and Battery .....	42
6.0	Conclusions.....	43
	Appendix—Fission Surface Power System Master Equipment List .....	45
	References.....	47

## List of Tables

Table 3-2.	—FSP Mass Summary .....	10
Table 4-1.	—Top-Level Reactor Performance Requirements .....	11
Table 4-2.	—Assumed FSP Reactor Criticality Requirements .....	12
Table 4-3.	—List of FSP Events/Transients Considered .....	13
Table 4-4.	—Primary Loop Volumes and Pressures at Various Conditions.....	22
Table 4-5.	—Preliminary Reactor Sensor List.....	25
Table 4-6.	—Reactor Module Power Losses .....	28

## List of Figures

Figure 2-1.	—FSP System for LAT2 option 6.....	4
Figure 2-2.	—Mars FSP concept. ....	4
Figure 2-3.	—Lander-integrated FSP system for LSS scenario 5.....	5
Figure 2-4.	—Scenario 5 shielding options. ....	5
Figure 3-1.	—FSP concept layout.....	9
Figure 3-2.	—FSP concept schematic.....	10
Figure 4-1.	—Reactor module radial cross-section.....	17
Figure 4-2.	—Reactor module axial cut-away view. ....	17
Figure 4-3.	—Average core temperature distribution. ....	18
Figure 4-4.	—Reactor heat transport layout.....	20
Figure 4-5.	—Annular linear induction pump. ....	21
Figure 4-6.	—NaK volume accumulator.....	22
Figure 4-7.	—Intermediate heat exchanger concept. ....	23
Figure 4-8.	—Control drive motor assembly.....	25
Figure 4-9.	—Buried shield layout. ....	27
Figure 4-10.	—Reactor power density contours. ....	28
Figure 5-1.	—Relative performance of various power conversion options. ....	30
Figure 5-2.	—Stirling hot-side heat exchanger options. ....	31
Figure 5-3.	—International Space Station heat rejection system. ....	33
Figure 5-4.	—Radiator panel cross-section.....	33
Figure 5-5.	—12 kWe dual-opposed Stirling convertor.....	34
Figure 5-6.	—Stirling hot-side heat exchanger concept.....	35
Figure 5-7.	—Heat transport schematic. ....	36
Figure 5-8.	—Second generation RDU manifold concept. ....	37
Figure 5-9.	—Lunar sink temperature variations and resulting FSP performance. ....	38
Figure 5-10.	—Radiator assembly (1 of 5 per wing). ....	39
Figure 5-11.	—FSP radiator deployment mechanisms. ....	39
Figure 5-12.	—PMAD electrical schematic.....	41
Figure 5-13.	—LPC enclosure and radiators. ....	41
Figure 5-14.	—Estimated FSP startup profile.....	42

# **Fission Surface Power System Initial Concept Definition**

Fission Surface Power Team  
National Aeronautics and Space Administration  
and Department of Energy

## **Executive Summary**

Under the NASA Exploration Technology Development Program (ETDP) and in partnership with the Department of Energy (DOE), NASA has embarked on a project to develop Fission Surface Power (FSP) technology. The primary goals of the project are to 1) develop FSP concepts that meet expected surface power requirements at reasonable cost with added benefits over other options, 2) establish a hardware-based technical foundation for FSP design concepts and reduce overall development risk, 3) reduce the cost uncertainties for FSP and establish greater credibility for flight system cost estimates, and 4) generate the key products to allow NASA decision-makers to consider FSP as a preferred option for flight development.

The FSP project was initiated in 2006 as the Prometheus Program and the Jupiter Icy Moons Orbiter (JIMO) mission were phased-out. As a first step, NASA Headquarters commissioned the Affordable Fission Surface Power System Study to evaluate the potential for an affordable FSP development approach. With a cost-effective FSP strategy identified, the FSP team evaluated design options and selected a Preliminary Reference Concept to guide technology development. Since then, the FSP Preliminary Reference Concept has served as a point-of-departure for several NASA mission architecture studies examining the use of nuclear power and has provided the foundation for a series of “Pathfinder” hardware tests. The long-term technology goal is a Technology Demonstration Unit (TDU) integrated system test using full-scale components and a non-nuclear reactor simulator.

The FSP team consists of Glenn Research Center (GRC), Marshall Space Flight Center (MSFC) and the DOE National Laboratories at Los Alamos (LANL), Idaho (INL), Oak Ridge (ORNL), and Sandia (SNL). The project is organized into two main elements: Concept Definition and Risk Reduction. Under Concept Definition, the team performs trade studies, develops analytical tools, and formulates system concepts. Under Risk Reduction the team develops hardware prototypes and conducts laboratory-based testing.

## **1.0 Purpose**

The purpose of this document is to describe the Fission Surface Power (FSP) Initial Concept that has resulted from trade studies and design decisions made by the FSP team between January 2008 and June 2009. It specifically addresses the current status of the FSP system design as developed under the Concept Definition project element. The document does NOT address the various other project activities that contribute to the overall FSP technology maturation such as analytical modeling, hardware testing, and TDU development.

The primary goals of the Concept Definition effort are to generate reference concepts to guide FSP hardware development and to support Lunar Surface System (LSS) architecture studies by providing credible and timely FSP design information. The FSP system design described in this document is considered at the Pre-Phase A stage. The design will continue to evolve as requirements are better defined and hardware testing is completed. If flight system development is authorized, industrial contractors would refine the FSP design and potentially select different details from those presented here. However, the major technology building blocks being developed in the current project are expected to provide the basis for the detailed flight design.

## 1.1 Affordable Fission Surface Power System Study

One of the major challenges to the implementation of space fission power systems is development cost. In April 2006, NASA and DOE initiated the Affordable Fission Surface Power System Study (AFSPSS) to determine the design features and expected costs of a representative FSP system. A government study team with members from several NASA field centers and DOE laboratories evaluated technology options and design variables and selected a reference concept based on affordability and risk. A low-risk approach was selected over other options that could offer higher system performance and/or lower mass. The team also defined a credible development schedule and generated a detailed Work Breakdown Structure (WBS)-based cost estimate.

The results indicated that the initial FSP system could be developed, flight-qualified, and delivered to the lunar surface by 2020 for approximately \$1.4 billion with follow-on systems costing about \$215 million each (Ref. 1).

## 1.2 Preliminary Reference Concept Selection

The “Affordable” design approach was considered representative of a number of potential system concepts. In order to determine a primary FSP reference concept, the team generated a comprehensive list of system design options and conducted screening studies that led to six plausible concepts for further study. All of the plausible concepts identified presumed the use of a low temperature (<900 K) reactor heat source with conventional materials as a path toward achieving an affordable solution. The plausible concepts included a liquid-metal cooled reactor with Stirling, Brayton, thermoelectric, or organic-Rankine power conversion, a gas-cooled reactor with Brayton power conversion, and a heat pipe cooled reactor with Stirling power conversion. The concepts were evaluated for performance and relative cost against a common set of mission requirements and development constraints derived from the earlier “Affordable” study. In 2008, a management review panel led by NASA Headquarters selected the liquid-metal reactor with Stirling power conversion as the FSP Preliminary Reference Concept and recommended Brayton as a back-up conversion option should unforeseen difficulties arise with the Stirling technology development efforts (Ref. 2).

The resulting Preliminary Reference Concept includes a liquid-metal cooled, fast-spectrum reactor with Stirling power conversion and water-based heat rejection (Ref. 3). The reactor uses  $\text{UO}_2$  fuel pins in a hexagonal core with an external radial reflector and control drums. Heat is transferred to the Stirling power convertors by a pumped sodium-potassium (NaK) reactor cooling loop. The core structure and coolant piping are constructed of stainless-steel to reduce cost and development risk. The radial reflector is beryllium in a stainless-steel shell. The control drums are beryllium and boron-carbide, also enclosed in stainless-steel. The reactor is located at the bottom of an approximate 2 m deep excavation. The lunar regolith limits radiation from the reactor to less than 5 rem/yr at a 100 m radius. The Stirling convertors generate single-phase ac electric power that is converted to dc for user loads. Stirling waste heat is removed by a pumped water cooling loop that is coupled to a series of two-sided, vertical radiator panels. The radiator panels are comprised of titanium-water heat pipes in a composite facesheet sandwich. The FSP concept is designed to produce a net power of 40 kWe with a full-power service life of at least 8 years. This same technology could be used for missions at essentially any location (equator to poles) on the lunar or Mars surface.

## **2.0 Lunar and Mars Architecture Studies**

Beginning with the Exploration Systems Architecture Study (ESAS) in 2005, NASA has conducted various mission architecture studies to evaluate implementation options for the U.S. Space Policy (formerly the Vision for Space Exploration). Several of the studies examined the use of fission power systems for human missions to the lunar and Martian surface. The FSP team contributed by supplying FSP design characteristics, developing mission-compatible configuration options, and defining a Concept-of-Operations consistent with the mission objectives.

### **2.1 Lunar Architecture Team**

In 2007, the second phase of the Lunar Architecture Team (LAT2) developed an FSP-based architecture known as Option 6 for a polar lunar outpost at the Shackleton Crater site. The nuclear-based architecture was proposed to accelerate outpost buildup, achieve earlier 180-day missions, and maximize the total number of crew days on the surface. Option 6 uses the buried reactor concept delivered on a cargo lander and installed by a combination of robots and crew, as shown in Figure 2-1. An earlier lander delivers a small solar array and battery to supply initial power, the FSP Power Management and Distribution (PMAD) equipment, and a bladed-rover that prepares the site for the reactor. Once installed, the FSP system provides a robust power capability of 40 kWe resulting in substantial power margin for early outpost build-up and operations. It also provides capacity for power increases associated with the initial surface elements and the potential for expanded science and resource utilization. System trades comparing Option 6 to similar LAT2 architectures with solar photovoltaic (PV) arrays and regenerative fuel cells (RFC) showed the FSP-based architecture to offer significantly more power with less power system mass and comparable cost despite the favorable conditions for solar power at Shackleton.

A key question raised about the FSP installation was the feasibility of excavating the reactor hole. Supporting studies were conducted by the in-situ resource utilization (ISRU) team during LAT2 to evaluate methods for excavating a 2 m deep hole. The study evaluated various digging methods and developed analytical models to predict the mass and power requirements for the machinery. It was determined that the process could use the same semi-automated regolith-moving equipment planned for the ISRU oxygen production plant. The recommended approach was to prepare an oversized hole with a ramp that could accommodate ingress/egress of a bladed-rover. Preliminary estimates indicated the need to move about 24 m<sup>3</sup> of regolith, including the final backfilling of the ramp, over a time period of 41 to 50 days.

### **2.2 Mars Architecture Team**

During the same time period, the Mars Architecture Team (MAT) was reviewing power system options for a crewed mission to Mars. The basic architecture was derived from previous Mars mission concepts in which an initial cargo lander delivers a power system and ISRU plant to locally produce the return propellant before the crew ever leaves Earth. A nuclear system allows the propellant production to be completed faster and more efficiently through continuous day/night operations. The power requirements for the nuclear power option were about 30 kWe during the pre-crew deployment phase and about 20 kWe after the crew arrives. The 30-kWe power level was similar enough to the reference 40 kWe lunar concept that no power system design changes were required. The MAT-based FSP concept assumed the reactor on a mobile cart with integral shielding that is robotically deployed from the lander, as shown in Figure 2-2. The above-grade reactor configuration was chosen for this application because the MAT wanted to avoid digging operations. FSP was selected as the baseline power system for MAT based on advantages in system mass, operational flexibility, and environmental robustness as compared to solar power systems with energy storage (Ref. 4).

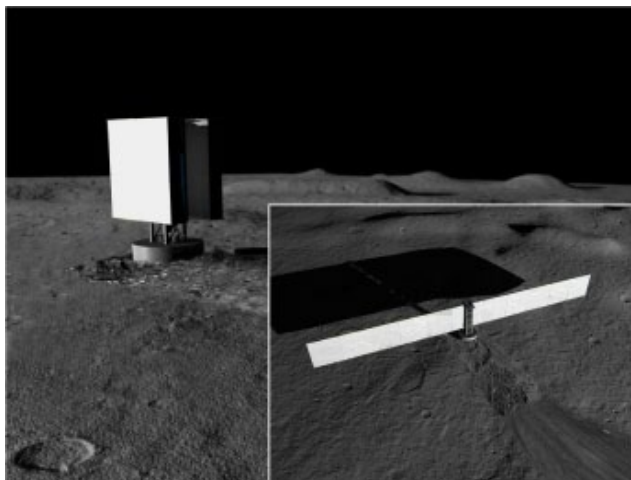


Figure 2-1.—FSP System for LAT2 option 6.

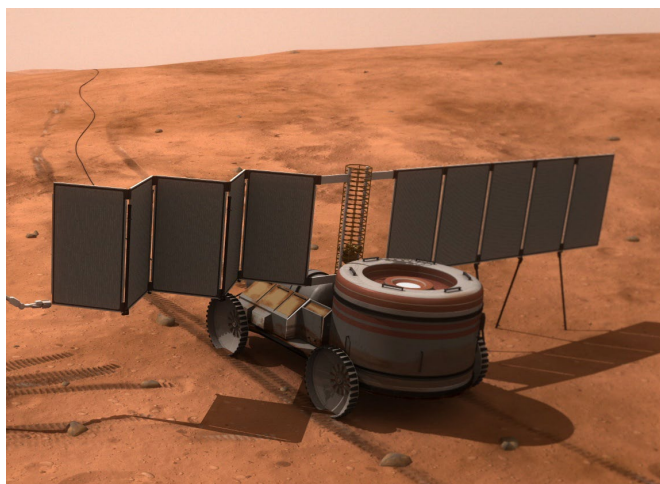


Figure 2-2.—Mars FSP concept.

## 2.3 Lunar Surface Systems

In 2008, Lunar Surface Systems (LSS) and the Constellation Architecture Team developed an FSP-based architecture known as Scenario 5. Two basic FSP options were investigated including the typical off-loaded and buried system and a new concept where the FSP system remained on the lander, as shown in Figure 2-3. In either case, the FSP system was to be delivered on the first cargo lander to provide a power-rich environment for early outpost buildup. Both systems also assumed a central power distribution node at the outpost. This provided an easy-access power bus for outpost loads such as habitats, ISRU equipment, rover recharging, and science experiments. It also placed the FSP system's power and control electronics at a location that was readily accessible should maintenance be required. A small Orion-based solar array (5 kWe) and battery (30 kW-hr) was included with the FSP PMAD for startup and emergency backup. A follow-on architecture evaluated by LSS, referred to as Scenario 12, included an FSP system that was delivered later in the lunar campaign using a similar design approach.

The FSP team did an extensive evaluation of radiation shielding options to support the architecture definition (Ref. 5). Figure 2-4 shows graphical representations of the Monte-Carlo N-Particle (MCNP) transport code models developed for the four shielding approaches that were examined including: A) FSP system off-loaded and reactor buried, B) FSP system off-loaded and placed on surface with surrounding regolith berm, C) FSP stays on the lander as delivered from Earth, and D) FSP system stays on the lander with regolith shielding augmentation.

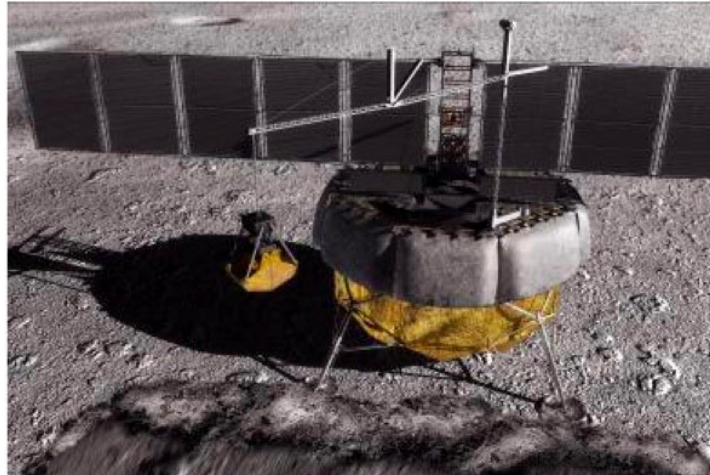


Figure 2-3.—Lander-integrated FSP system for LSS scenario 5.

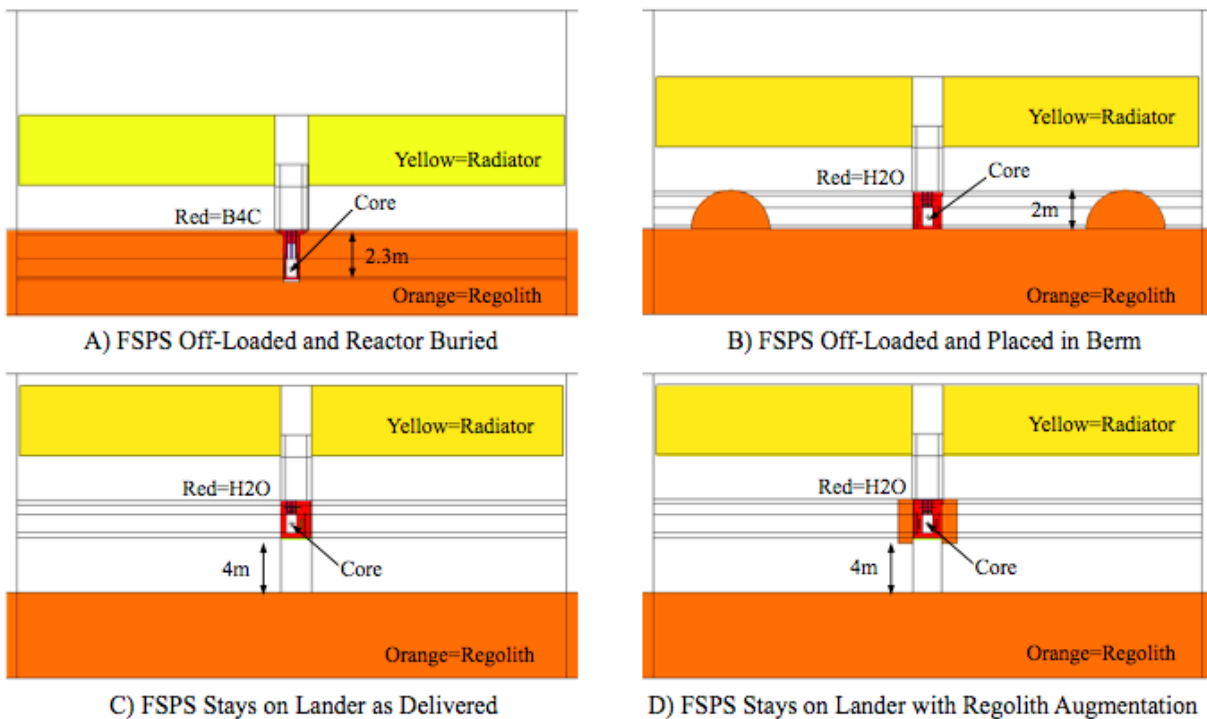


Figure 2-4.—Scenario 5 shielding options.

All options assumed a 3 mrem/hr (26.3 rem/yr) reactor dose rate to an unshielded astronaut at a specified separation distance. This is higher than the 5 rem/yr dose previously mentioned in order to account for more realistic crew routines and schedules. Crew length-of-stay is expected to be no greater than 180 days with the majority of time spent in shielded habitats and rovers away from the hypothetical reactor boundary. Given reasonable assumptions for crew operations, the total radiation to a crew member from the reactor based on the 3 mrem/hr dose rate at the specified distance is expected to be considerably less than 5 rem per year of duty. The actual allowable astronaut radiation dose is not defined yet and will depend on many factors including natural radiation levels, proximity to nuclear sources (such as FSP), crew shielding, length of mission, and Extra-Vehicular Activity (EVA) duty cycle. The FSP-related dose is expected to be a small percentage of the total received by crew members during their lunar stay. The

FSP shielding must also protect its own components located on the truss above the shield. The assumed dose limits for truss-mounted equipment above the shield were 5 Mrad (gamma) and  $2.5 \times 10^{14}$  nvt (neutrons), although these values are subject to change as irradiation tests are performed on FSP components and materials. In most cases, the FSP equipment was the limiting factor in determining the required FSP shield mass.

The buried reactor case (A) resulted in a 2080 kg delivered shield, predominantly boron-carbide ( $B_4C$ ), with the reactor core buried to a 2.3 m depth. This approach offered the shortest separation distance among the options at 100 m. It also offers the lowest delivered shield mass, and this could be further reduced by using water rather than  $B_4C$ . The berm shield case (B) assumed a 2 m tall regolith berm surrounding the reactor. It resulted in a 2660 kg delivered shield using water and depleted uranium (DU) and a 200 m separation distance. The landed shield cases (C and D) assumed the reactor remained in the central lander cavity between the propellant tanks at a height of approximately 4 m above the lunar surface. The “as-delivered” lander case (C) required a shaped shield of water and DU that was thicker in the direction of the outpost. It was still the heaviest delivered shield at 2980 kg and required a separation distance of 1000 m. The regolith-augmented lander case (D) resulted in a 2250 kg delivered shield mass of water and DU supplemented with 0.8 m thick regolith-filled annulus surrounding the water vessel and a 400 m separation distance.

The separation distances for the various shield options were determined in conjunction with power transmission cable mass estimates. Generally, there is an optimum distance that balances shield mass and cable mass. Table 2-1 provides a summary of the power transmission assumptions and resulting cable masses for the four cases. Larger distances require more elaborate power transmission approaches. In all cases, the power distribution node was assumed to be located at the specified separation distance and a 25 percent margin was added for cable length. The cable bundle was assumed to include a main power cable, auxiliary power cable (for FSP parasitic loads), and a data transmission cable (for FSP instrumentation signals). The main power cable includes parallel channels for each of the eight Stirling alternators. The auxiliary power cable is assumed to carry a total of 5 kWe via 10 parallel channels.

TABLE 2-1.—SCENARIO 5 POWER TRANSMISSION ANALYSIS

Shield option	A	B	C	D
Separation distance, m	100	200	1000	400
Cable length, m	125	250	1250	500
Transmission, Vac	400	400	2000	400
Auxiliary bus, Vdc	120	120	120	270
Auxiliary bus location	Outpost	Outpost	FSP	Outpost
Main power cable, kg	48	128	688	400
Auxiliary power cable, kg	120	450	120	300
Data cable, kg	12	32	12	100
High voltage transformers, kg	-----	-----	144	-----
Total transmission mass, kg	180	610	964	800

Cases A and B assumed direct 400 Vac power cabling from the Stirling alternators to the power distribution node where the 400 Vac was converted to 120 Vdc for the user load bus. The same 120 Vdc bus was used to power FSP parasitic loads, such as pumps and motors, via a power cable from the distribution node back to the FSP system. The larger separation distance for Case C required the addition of high voltage transformers near the FSP system to boost the transmission voltage to 2000 Vac. 2000 Vac provides a reasonable compromise on cable mass, development risk, and operational complexity. The 120 Vdc auxiliary power bus and FSP data bus was assumed to be co-located with the transformers at a 100 m distance from the FSP system. Case D assumed direct 400 Vac transmission, a 120 Vdc user load bus, and a 270 Vdc auxiliary power bus and return cable.

The LSS and Constellation Architecture Team settled on two FSP configurations for Scenario 5. The two systems used the same reactor, power conversion, heat rejection, and PMAD equipment. The off-loaded configuration assumed the use of the “ATHLETE” utility rover for excavating a hole, off-loading

the FSP system from the lander, transporting it to the site, and positioning it in the hole. The total FSP system mass was about 5800 kg including shielding and cabling. The integrated landed configuration assumed the regolith-augmented shield with the lander cavity filled using a crane that scoops regolith collected near the lander by a bladed-rover. The total FSP system mass was about 6600 kg with shielding and cabling.

### **3.0 FSP System Overview**

The FSP system is defined by four major elements: (1) Reactor Module, (2) Power Conversion Module, (3) Heat Rejection Module, and (4) Power Management and Distribution (PMAD) Module. The reactor generates the nuclear heat through fission. Thermal power is transferred from the reactor to the power conversion and waste heat is transferred from the power conversion to the heat rejection. Electrical power generated by the power conversion is processed through the PMAD to the user loads. The PMAD supplies electric power for power conversion startup and for auxiliary loads associated with the reactor and heat rejection. The PMAD also provides the primary communications link for command, telemetry, and health monitoring of the FSP system.

#### **3.1 Derived Requirements**

Table 3-1 presents a summary of the top-level requirements developed for the FSP system. The requirements are termed “derived” because they were predominantly defined by the FSP team in response to suggestions by NASA Headquarters and the various NASA architecture study teams. Many of the FSP safety-related requirements were generated by the FSP team based on previous space fission system development projects, such as SP-100 and JIMO. These requirements will undoubtedly be reviewed (and perhaps expanded) by independent design experts once FSP reaches flight development status. For now, they provide a reasonable starting-point to guide FSP concept definition and technology development.

The key requirements that drive FSP system design are power level and service life. The 40 kWe power output is consistent with numerous studies that have estimated power requirements for the initial phase of a human lunar outpost dating back to the 1990’s Space Exploration Initiative and before. That power level is also well suited for an initial space reactor because it is large enough to demonstrate the mass-effectiveness of nuclear fission, but not too large to over-complicate the design and development process. In actuality, the fission technology developed for the 40 kWe design is readily scalable between 10 and 100 kWe. Below 10 kWe, the mass and cost advantages of fission power systems are not as compelling. Above 100 kWe, the reactor and power conversion technologies selected for FSP may need to be re-evaluated.

The 8 year service life also represents a reasonable balance of performance and risk. It is long enough to accommodate most estimates for lunar and Mars surface mission duration. For longer missions, it would be prudent to utilize multiple FSP units and stagger their delivery to provide overlap. The 8 year design life is also well within current technology projections for low temperature liquid metal reactors and dynamic power conversion. In addition, notional FSP development schedules indicate that sufficient qualification testing can be performed to demonstrate 8 year life while still meeting the proposed launch date.

System mass is another requirement that could influence FSP design. The current derived requirement is that the FSP system mass be less than the payload capacity of the lander. The current cargo lander concept is projected to deliver approximately 14000 kg to the lunar surface. The 40 kWe FSP system can easily be accommodated within this mass constraint, and most estimates show the system to be less than one-half of the lander cargo capacity. The generous lander payload allocation eliminates system mass as a major FSP design driver and allows the system to utilize low risk technology to minimize development cost and increase system reliability. Nevertheless, the FSP system design incorporates various mass saving features in order to maximize the mass available for other payloads. This also assures that the concept is relevant for future applications that may be more mass-constrained.

TABLE 3-1.—FSP DERIVED REQUIREMENTS

Requirement	Rationale	Source
1. The FSPS shall be designed to produce no less than 40 kWe net power output (after accounting for all power losses and auxiliary loads).	Provides sufficient power for extended-stay crew habitation, ISRU production facilities, rover recharging, and science equipment, including margin.	ESAS, LAT2
2. The FSPS shall be designed for use at any location on the lunar surface. Radiator sizing shall be based on worst-case surface temperatures and Sun angles.	Provides maximum flexibility in locating the lunar outpost. (The preferred lunar outpost location has not been determined.)	AFSPSS
3. The FSPS shall be designed to operate for no less than 8 years at full power.	Provides maximum service life without introducing excessive risk in FSP development and qualification.	AFSPSS
4. The FSPS shall be flight-ready for an initial launch and deployment no later than 2022.	Assures FSPS availability for initial outpost deployment based on current lunar emplacement schedules.	LAT2, LSS
5. The FSPS shall be designed to produce no less than 50 percent power output after the first credible component failure.	Assures FSPS power availability to meet essential crew power requirements following a component failure.	AFSPSS, LAT2
6. The FSPS shall be recoverable from all credible operational upsets and transients without adverse safety consequences to the crew or outpost.	Assures FSPS power availability following an off-nominal event and a return to safe FSP operation.	AFSPSS
7. The radiation from the FSPS shall be less than 5 rem/yr to an unshielded crew member located at the outpost.	Provides a guideline for FSPS shield design that corresponds to 10% of the astronaut annual dose limit. (The allowable crew dose from the FSPS has not been determined.)	AFSPSS, LAT2
8. The reactor shall remain subcritical during all planned and credible unplanned mission events prior to FSPS startup.	Assures that the FSPS does not present a radiological safety hazard before initial startup is commanded.	AFSPSS
9. At its end-of-life, the reactor shall be decommissioned in a safe shutdown condition.	Assures that the FSPS does not present a human safety hazard after final shutdown is commanded.	AFSPSS
10. The FSPS mass shall be minimized and no greater than the current cargo lander down-mass capability of 14000 kg.	Permits the FSPS to be delivered as a fully integrated package with available cargo mass to accommodate other payloads.	LAT2, LSS
11. The FSPS design shall be extensible to the Mars surface. All materials and design strategies shall be compatible with the Martian environment.	Provides maximum return on FSPS technology investment by designating its applicability for both the Moon and Mars.	LAT2, MAT
12. The FSPS shall be designed for robotic deployment using tele-operation.	Permits the FSPS to be installed at the lunar outpost without local human assistance, but does not preclude it.	LAT2, MAT, LSS

ESAS = Exploration Systems Architecture Study (2005), AFSPSS = Affordable Fission Surface Power System Study (2006), LAT2 = Lunar Architecture Team, 2<sup>nd</sup> Phase (2007), MAT = Mars Architecture Team (2007), LSS = Lunar Surface Systems (2008).

### 3.2 Design Summary

The preliminary reference concept layout is shown in Figure 3-1. The reactor core is located at the bottom of an approximate 2 m deep excavation with an upper plug shield to protect the equipment above from direct radiation. The NaK pumps, Stirling converters, and water pumps are mounted on a 5 m tall truss structure that attaches to the top face of the shield. Two symmetric radiator wings are deployed via a scissor mechanism from the truss. Each radiator wing is approximately 4 m tall by 16 m long and is suspended 1 m above the lunar surface. In its stowed configuration, the FSP system is approximately 3 by 3 by 7 m tall.

The buried configuration was selected for the preliminary reference concept because it minimizes the mass of radiation shielding that must be delivered from Earth. It also simplifies the PMAD because the buried reactor can be located relatively close to the outpost to shorten transmission cable length. There are numerous other FSP installation options (such as those shown in Fig. 2-4) that could be developed depending on mission needs. The basic technology building blocks of the liquid metal cooled reactor, Stirling power conversion, and water-based heat rejection would be essentially the same. The decision on FSP configuration can easily be deferred until the flight program since most of the design challenges related to the configuration are engineering-based rather than technology-based.

The preliminary reference concept schematic is shown in Figure 3-2. The use of redundant components and parallel fluid loops allows the system to produce partial power in the event of unexpected failures. The schematic shows the system energy balance and the anticipated temperatures, pressures, and flow rates at some of the key interfaces.

The reactor (Rx) produces 186 kWt with a peak fuel pin clad temperature of 860 K. It delivers heated NaK at 850 K to a pair of intermediate heat exchangers (IHX) using two fully-redundant electromagnetic primary pumps (PP). The IHX is a NaK-to-NaK heat exchanger that provides a buffer between the primary NaK and the Stirling converters, and a means to adjust the NaK flow rate and resulting temperature drop across the Stirling converters separately from the reactor flow and temperature drop. Each intermediate NaK loop services two Stirling converters at a supply temperature of 824 K. The effective Stirling hot-end cycle temperature is 778 K. The secondary NaK loops include an intermediate electromagnetic pump (IP) of similar design to the primary NaK pump.

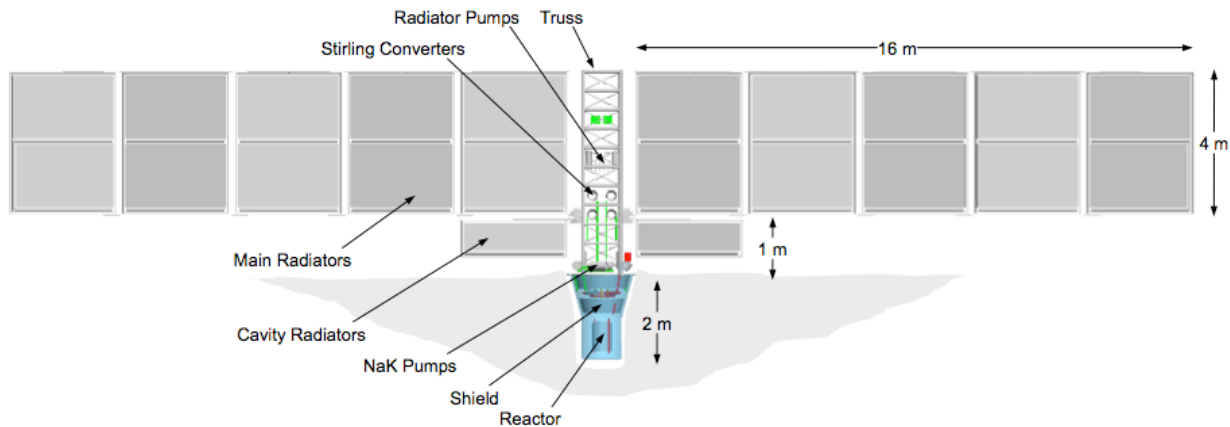


Figure 3-1.—FSP concept layout.



## 4.0 Reactor Module

The reactor module consists of the core, reflector, heat transport, instrumentation and control, radiation shielding, and thermal control. The most important factor in developing an affordable FSP reactor concept is to work within the bounds of established materials and available technologies. The reference FSP system is a stainless-steel,  $\text{UO}_2$ , pumped-NaK cooled reactor with Stirling power conversion and pumped-water heat rejection. For this study, design decisions were heavily weighted to assure safety and mission success. The reference reactor poses no significant radiological risk prior to reactor operation; therefore, the only nuclear safety issue is to avoid inadvertent criticality during ground handling, launch, lunar transport, and emplacement. To simplify criticality safety, the system is designed such that there is no credible scenario that results in criticality other than the control elements moving into their operational positions. Beyond safety considerations, reactor design decisions were made to simplify development and lower cost as opposed to increase performance.

The FSP reactor has an overall negative-temperature coefficient of reactivity. This means that the reactor power will self-regulate to match the power demanded in a manner that keeps the reactor temperature essentially constant. Therefore the reactor can inherently respond to any power conversion operational changes (e.g., convertor shutdown, electrical power reduction, etc.) by automatically adjusting fission power. Other sources of energy production within the core (mainly decay heat from unstable fission isotopes) will be managed by passive heat transfer paths designed into the reactor module. The FSP system can operate safely without continuous operator attention during normal full power operation and, to the extent possible, the system is designed to accommodate unanticipated malfunctions without requiring a control system response.

The top-level reactor performance requirements are shown in Table 4-1. There is a strong interdependency between the system and reactor requirements; e.g., the reactor thermal power is based on a certain pump efficiency, thus a change in reactor pump efficiency would change the reactor thermal power level. The requirements for the dose above the shield represent the average dose integrated over 8 years within the open volume. If some components require a lower dose, then they can be spot shielded and/or placed in the locations within this region that have a lower than average dose. As mentioned previously, the astronaut dose limit attributed to the reactor is very mission dependent, but is assumed to be less than 5 rem per year to an individual crew member during their tour of duty. There is ample margin in the reactor design to accommodate requirement changes without a major deviation to the reactor and FSP system design.

TABLE 4-1.—TOP-LEVEL REACTOR PERFORMANCE REQUIREMENTS

Parameter	Value
Thermal power	186 kWt
Full-power system lifetime	8 years
Silicon gamma dose (above shield)	5 MRad
Fast neutron fluence (above shield)	2.5e14 nvt

Some of the criticality requirements assumed for this design concept are shown in Table 4-2. The first requirement is to ensure there is sufficient margin in the FSP reactor to maintain criticality throughout lifetime, in both warm and cold temperature conditions. A 2 percent margin ( $k\text{-eff } 1.02$ ) is meant to address uncertainties in nuclear cross section data, computational/code uncertainties, material density/isotopic uncertainties and geometry uncertainties. These, or similar margins will remain in place until nuclear criticality testing better quantifies the uncertainties. The second requirement is to allow 0.5 percent margin ( $k\text{-eff } 1.005$ ) for criticality in all cases even when one control drum is stuck in its lowest reactivity (stowed) position. This requirement is to allow for the contingency that one control drum within the radial reflector will fail to move after launch and emplacement. The third requirement is to ensure that the reactor will remain subcritical for all transportation, handling, and storage operations prior to launch.

TABLE 4-2.—ASSUMED FSP REACTOR  
CRITICALITY REQUIREMENTS

Configuration	k-eff
Drums out (BOL-EOL, Cold-Warm)	>1.020
One drum stuck in (BOL-EOL, Cold-Warm)	>1.005
Drums in (BOL-EOL, Cold-Warm)	<0.950
Evaluated accident scenarios	<0.985

The fourth requirement is to ensure that the reactor remains subcritical during all credible postulated launch accidents. For this requirement, there are numerous environments and configurations evaluated. There is no basis to imply that any or all of the evaluated scenarios are credible from a launch safety perspective; rather, they are evaluated to provide confidence that the concept should remain subcritical during what might eventually be deemed a credible scenario.

The launch accident scenario analysis examined 42 unique cases. There were three reactor environments evaluated: a) reactor internal voids filled with NaK and external voids filled with dry sand, b) reactor internal voids and external voids filled with fresh water, resting on concrete, and c) reactor internal voids filled with sea-water and external voids filled with wet sand. Dry sand is assumed to be pure quartz at 64 percent theoretical density. Wet sand is assumed to be 64 percent quartz, 36 percent seawater with a composite density of 2.06 g/cm<sup>3</sup>. In all cases the surrounding material is assumed to be infinitely thick to neutrons. There were two reflector configurations evaluated: 1) radial reflector and control drums and all surrounding material removed (i.e., bare vessel), and 2) radial reflector and control drums intact (although possibly compacted), with drums in launch position. The environments and reflector states listed above lead to six cases (a1, a2, b1, b2, c1, c2) for each reactor configuration considered. The reactor configurations were: A) nominal, B) flood all internal pin gaps, C) compact radial reflector to eliminate gap between vessel and radial reflector, D) compact radial reflector and vessel to force all pin/wire gaps to close, E) compact further to force pin-to-pin contact (P/D = 1, wires crushed), F) compact further to crimp clad around fuel (eliminate fuel/clad gap), and G) compact further to eliminate all core void. Analysis of the 42 potential accident cases (i.e., a1A, a2A, b1A, ..., c1G, c2G) showed that the reactor remained subcritical for all cases with k-eff less than 0.985, and that most cases resulted in k-eff much less than 0.985. The only cases that approached 0.985 were those with a flooded reactor and the radial reflector/drums intact. If necessary, k-eff can be lowered in such cases by increasing the thickness or arc-length of the B<sub>4</sub>C poison layer in the drum.

Given the decision to use a compact fast spectrum reactor, the integral and major component reactivity feedback coefficients are well characterized and consistently negative. No explicit requirements have been imposed on the magnitude of reactor feedback coefficients or nuclear kinetic parameters, other than that the system responds to design-basis events with an acceptable, predictable, and stable dynamic response. Thermal-structural requirements are not formalized at this stage in the design process, beyond what might be considered standard engineering practice; e.g., primary stresses to 1/3 ultimate, 2/3 yield, creep limits of 1 percent, materials with at least 5 percent uniform elongation, temperature limits based on material/corrosion data, etc.

System transient analysis is an important part of the FSP design process. An additional benefit of a fast-spectrum reactor is that the use of point kinetic theory (in a lumped parameter model) can be very accurate for predicting transient reactor flux/power response. This greatly simplifies transient modeling and predictions, making it easier to qualify models and benchmark against warm-criticality experiments. The determination of electrical input power for a resistance-heated core simulator is also straightforward, making non-nuclear testing more realistic. In addition to modeling reactor startup, the design events and transients listed in Table 4-3 have been considered and/or analyzed to assess system response.

TABLE 4-3.—LIST OF FSP EVENTS/TRANSIENTS CONSIDERED

Component	Events/Transient to evaluate
Control drums	<ul style="list-style-type: none"> <li>• 1 of 6 drums stick at startup</li> <li>• All drums stick after achieving full power</li> </ul>
NaK pressure boundary	<ul style="list-style-type: none"> <li>• Loss of coolant in primary loop</li> <li>• Loss of coolant in one intermediate loop</li> </ul>
Primary pump	<ul style="list-style-type: none"> <li>• Primary flow drops by 50 percent</li> <li>• Pump failure followed by startup of backup pump</li> </ul>
Intermediate pump	<ul style="list-style-type: none"> <li>• 1 of 2 intermediate pumps fail</li> </ul>
Stirling convertor	<ul style="list-style-type: none"> <li>• 1 of 4 Stirling convertors fail</li> <li>• All Stirling convertors reduced to 80 percent of full piston stroke</li> </ul>
Radiator loop	<ul style="list-style-type: none"> <li>• 1 of 4 radiator loops fail</li> </ul>
Radiator	<ul style="list-style-type: none"> <li>• All radiators are coated with a thin layer of lunar dust</li> </ul>
Lunar environment	<ul style="list-style-type: none"> <li>• Lunar day/night thermal cycle</li> </ul>

## 4.1 Key Nuclear Design Decisions

### 4.1.1 Nuclear Fuel Selection

The nuclear fuel (i.e., fissile material) is often the most important technology decision for a space reactor. The selection is highly dependent on the desired system specific mass (kg/kW) and lifetime. A low specific-mass requirement leads to the selection of a high-temperature, high-uranium loading fuel that has good fission gas retention. Uranium-nitride (UN) has generally been the material of choice in this regime because of its high temperature potential and good fuel density, although it still requires significant development and infrastructure cost. Since specific mass is not a major driver for the FSP application, UO<sub>2</sub> offers a significantly lower cost and lower risk solution because it is the most widely used reactor fuel material today. While commercial reactors utilize this material in their fuel systems, the clad temperatures seldom exceed 600 K, well below the desired operational regime for space reactors. However, in the past, tens of thousands of oxide fuel rods were used in the Experimental Breeder Reactor (EBR)-II and Fast Flux Test Facility (FFTF) liquid metal reactors at clad temperatures exceeding 900 K.

A low-temperature surface application also invites the use of another fuel type with similar development maturity as UO<sub>2</sub>, namely uranium-metal fuels such as UZr and UMo. Metal fuels were considered a potentially affordable path because of the large database of fuel performance in EBR-II at temperatures and fuel burnup comparable to the FSP design. The reactor fuel used on the U.S. SNAP-10A reactor flown in 1965 was UZrH. This was another fuel option that was briefly considered for FSP but dismissed because of unproven life at the planned operating temperatures and the need to develop or recapture the hydrogen retention barrier technology. A thorough comparison was made between UO<sub>2</sub> and U-10Zr (10 percent Zr) for the FSP reference system, based upon the fuel performance characteristics required for this reactor system. As a result of this assessment, oxide fuel was selected as the preferred fuel form for the FSP reactor system, recognizing that U-10Zr is a possible alternative that would require similar development cost and schedule.

### 4.1.2 Structural Material Selection

Structural material selection (most notably the fuel clad) goes hand-in-hand with the fuel selection and development. In many cases it is better to consider the fuel and clad in tandem as the “fuel system”, but in this case it is discussed separately since it is highly desirable to have the fuel clad be the same material as the remainder of reactor structure (so that there are no dissimilar metals in contact with each other or the reactor coolant). The demands placed on a space reactor structural material are highly dependent on temperature, power, and lifetime. For a space reactor several attributes can be extremely

important: yield/ultimate strength, creep strength, ductility (especially under irradiation), fracture toughness, chemical compatibility, density, neutronics, modulus of elasticity, and ductile-to-brittle transition temperature (especially as it pertains to launch temperature). These attributes, in combination with the availability, fabricability, and weldability of the material, can be extremely challenging.

In previous space reactor programs, the system specific-mass requirement drove the reactor to a high operating temperature that often led to a refractory alloy solution and high materials development cost. However, if the peak coolant temperature can be kept below 900 K, it allows the use of stainless-steel alloys (304 and 316), which are widely used in terrestrial reactors and well characterized in radiation environments. Stainless-steel alloys are widely produced and are readily fabricable into the parts and structures a FSP reactor would require. As a result of the material assessment, Stainless Steel 316L was selected as the preferred structural material for the FSP reactor system, recognizing that other steels or nickel-based superalloys could be affordable alternatives depending on the final requirements of the system.

#### **4.1.3 Reactor Coolant Selection**

The coolant for the reference design is NaK-78 (78 percent K by mass). This selection is consistent with the SS-316 structural material selection in terms of both chemistry and allowable operating temperature. NaK is baselined because there is considerable experience with this coolant including all of the space reactor systems ever flown (SNAP-10A, BUK, and TOPAZ). The primary reason NaK is selected over other liquid metals such as sodium or potassium is its low freezing temperature of 262 K. All space reactor flight experience has been to “launch-liquid, stay-liquid”, and NaK makes this relatively straightforward. NaK is liquid at room temperature, and radiative heat losses are small enough at 262 K to require minimal heating (if any) in the space environment. The use of a coolant that is liquid at room temperature also simplifies test operations since freeze/thaw cycles can be avoided during startup and shutdown.

Past experience indicates that sodium and potassium are potential liquid metal coolant alternatives to NaK. Sodium has been used for nearly all of the terrestrial fast reactors. As compared to NaK, sodium has the advantages of higher specific heat (leading to reduced pumping power), lower vapor pressure, lower neutron capture, and less gas production. On the other hand, sodium has a freezing temperature of 371 K and a coolant activation that is three times that of NaK. Potassium has lower coolant activation, but higher gas production rates and less desirable fluid properties than NaK including a 337 K freezing temperature. Preliminary calculations have shown that the NaK coolant does not introduce radiation dose problems at the power conversion equipment and other components on the truss. The low freezing temperature, good fluid properties, and acceptable radiation characteristics makes NaK the preferred choice for FSP.

#### **4.1.4 Radial Reflector Material Selection**

The radial reflector material has a significant impact on the design of small, compact fast reactors like the FSP concept. A very “high-worth” reflector is needed not only to keep core size small, but also to more easily satisfy ground handling and launch safety requirements. The radial reflector material specified for most space reactors is beryllium (Be) or beryllium-oxide (BeO). All other candidate materials do not have a reactivity worth high enough to allow reasonable launch accident criticality requirements to be met without internal safety rods.

Be and BeO have rather complex behavior at high temperatures and neutron fluences. Fortunately, if the reactor power level and lifetime requirements are modest, then the radial reflector temperature and fluence levels can be relatively low ( $\sim 800$  K and  $<10^{20}$  n/cm<sup>2</sup> where  $E > 100$  keV). This alleviates many operational concerns associated with Be and BeO such as gas production, swelling, and embrittlement. The current FSP system requirements appear to be within the envelope for which beryllium performance is acceptable. The relatively low power and moderate design life of the FSP system would also reduce the likelihood of control elements bowing, sticking, or failing because of the lower fluence and thermal stress.

The reference reflector material selected for the FSP concept is beryllium. Be is generally a heavier option than BeO because of the lower macroscopic scatter cross-section, but Be is less susceptible to radiation/temperature induced swelling and cracking. Also, Be can better retain the high thermal conductivity required to transfer heat out of the system; including heat deposited directly into the radial reflector and heat radiated from the reactor vessel. One drawback of Be is that it produces more power peaking in the outer fuel pins due to a more thermalized spectrum returning from the radial reflector, but thermal-structural analysis has shown this peaking to be acceptable.

#### **4.1.5 Reactivity Control Mechanism Selection**

The FSP reactor is rather unique in both its reactivity requirements and the options available to control reactivity. First, the flight reactor is not subject to reactivity control requirements typically imposed on terrestrial systems (e.g., diverse and redundant shutdown). Second, the FSP reactor is very amenable to external reactivity control, either via leakage or absorption, because of high neutron leakage and the resulting high reactivity worth of the radial reflector. Third, the relatively small size of the FSP core allows the design to meet criticality requirements for all credible accident scenarios without an internal safety rod. Therefore, FSP reactor control can be accomplished with only one relatively simple form of external reactivity control.

External reactivity control can be accomplished by changing the neutron leakage rate and/or absorption rate in the radial reflector. Both options have been adopted on previous space reactor designs. Generally the reason for using a leakage-based system was to lower mass. For a surface fission system, leakage would significantly increase shielding mass because some type of 4-Pi shield configuration would likely be needed. Further, leakage control would not be as effective from a neutron standpoint because of backscatter from other components. Leakage could also create thermal-balance and component irradiation issues that would vary depending on the position of the control elements. For these reasons, the selected method for FSP reactivity control was neutron absorption, rather than leakage.

There were two options considered for FSP control elements: rotating control drums embedded in the radial reflector and sliding poison slats between the vessel and radial reflector. Reactivity evaluations found that both methods were similarly effective in providing the required reactivity control. In either case, the thermal design may be the greater engineering challenge. Both systems require the neutron reflector and absorber materials to operate at higher temperatures than typical terrestrial systems. A drum approach requires some of the Be to operate at high temperature because of the radiation gap between the drum and the radial reflector, which could pose thermal stress issues. The sliding poison option presents thermal balance concerns because it serves as a shutter with two radiation gaps, and the thermal design must account for any combination of shutter positions (i.e., from fully open to fully closed). The positional changes of the sliders and the resulting gaps also affect the radiation streaming and shield design. Each concept has unique requirements related to bearings and mechanisms, but these are primarily engineering issues that can be resolved in a flight development program. Both rotating and translating control elements have some limited flight heritage; however neither has been fully examined in the context of a modern launch safety analysis. As a result of the preliminary assessment, Be/B<sub>4</sub>C control drums were selected as the reference control mechanism for the FSP reactor system, recognizing that a sliding poison system could be made to work as well. A future more detailed evaluation of the reactivity control system is planned to make a more informed selection.

#### **4.1.6 Pump Technology**

Given the decision to use a pumped-liquid-metal reactor cooling system, the pump technology becomes a crucial design element. At the highest level, two basic methods may be considered to circulate the liquid metal: mechanical and electromagnetic (EM) pumps. EM pumps have numerous advantages including: 1) there are no shaft seals that might lead to liquid metal leakage, and 2) they have no moving parts and require no bearing lubrication. EM pumps are also radiation tolerant and have demonstrated operational lifetimes far in excess of the FSP design goal. Because of these advantages, EM pumps have

been selected for many liquid metal pumping applications. Mechanical pumps were omitted from consideration to avoid wear issues, mechanically induced vibration, radiation degradation, and sealing difficulties. The biggest drawback of EM pumps is low efficiency, but the efficiency advantages of a mechanical pump do not appear to justify the increased operational risks.

EM pump concepts can be divided into two categories: induction pumps and conduction pumps. The induction pump concepts may be further categorized by configuration: annular, flat and helical. The conduction pumps are either ac or dc powered, and the dc pumps are further divided into externally-powered and self-powered, i.e., Thermoelectric electromagnetic (TEM) pumps. EM pumps in each of these categories and subcategories have been designed, built, and successfully operated to circulate liquid metals for a broad range of applications. Of particular interest to this program are the Liquid Metal Fast Breeder Reactor (LMFBR) program pumps used to circulate Li, Na, and NaK. Based on prior experience and recent studies, an Annular Linear Induction Pump (ALIP) was selected as the FSP reference. The ALIP has the lowest mass of the induction pump family and has the simplest duct design. A major element of the current FSP technology project is dedicated to fabrication and testing of ALIPs.

## 4.2 Core and Reflector

The FSP reference reactor is designed to supply 186 kWt to the power conversion via pumped NaK coolant, and is designed for a full-power lifetime of 8 years. Many of the design choices for the reference system were made to simplify core neutronics and dynamic response. The neutron spectrum in the core is very hard (high average neutron energy level), which can eliminate many complicating reactor issues associated with thermal-spectrum reactors. There are no reactivity effects caused by buildup or decay of fission products (most notably Xe poisoning). The reactivity effects attributed to local non-heterogeneities or moderator temperature issues are also effectively eliminated. Cross-sections are well understood in the fast spectrum (most importantly U-235) and the reactivity effects due to cross-sectional changes with temperature are minor.

The compact geometry, in combination with the very hard spectrum, creates tight neutronic coupling within the core. Power and flux peaking factors are relatively low; the overall fuel peak-to-average power density is 1.50, the peak-pin-to-average-pin power is 1.23, and the average axial peaking factor is 1.22. The tight coupling also makes isolated local reactivity effects and/or spatial neutronic instabilities unlikely. As mentioned previously, one of the most significant benefits of the fast spectrum is that it allows the system to be designed without the need for in-core shutdown rods.

There are two unique aspects of this highly-reflected compact fast reactor that are not typical in larger terrestrial fast reactors. (1) The neutron reflector has a significant impact on dynamic performance, and in some cases the temperature coefficient of the radial reflector is higher than that of the fuel. The thermal time constant of the reflector is much longer than that of any component in the core, which requires reflector temperature and expansion effects to be modeled individually. (2) Reflected neutrons have a much longer lifespan than in-core neutrons. In effect, this creates additional delayed neutron groups, referred to as geometric delayed neutron groups. These groups can have lifespans that are orders-of-magnitude greater than neutrons that do not leave the core, and have much higher worth due to moderation. For compact beryllium reflected reactors there is also a measurable delayed group of photo-induced neutrons that result from delayed gamma interactions.

Figure 4-1 shows a radial cross-section through the mid-plane of the FSP core/reflector assembly. Figure 4-2 shows a 3D axial cutaway view. The majority of the neutronic, thermal, and mechanical design and analysis of this assembly is beyond the scope of this document. The following sections provide a brief description and document some of the key design features.

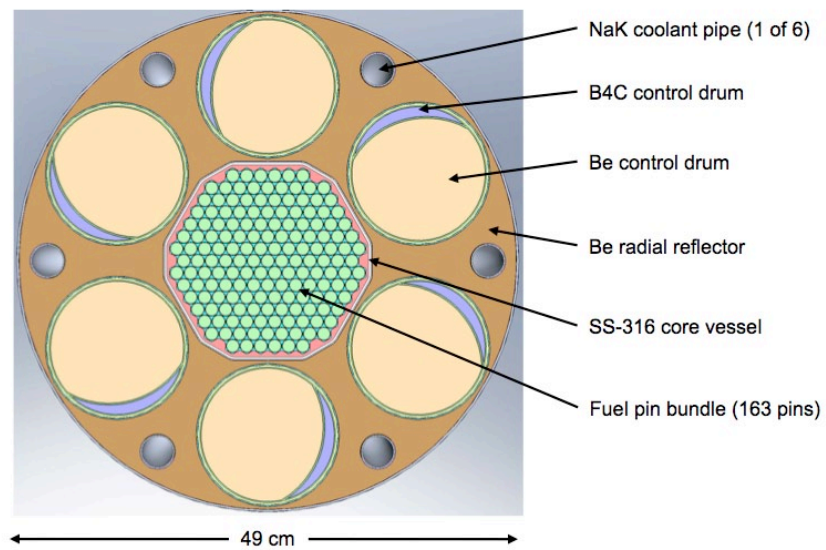


Figure 4-1.—Reactor module radial cross-section.

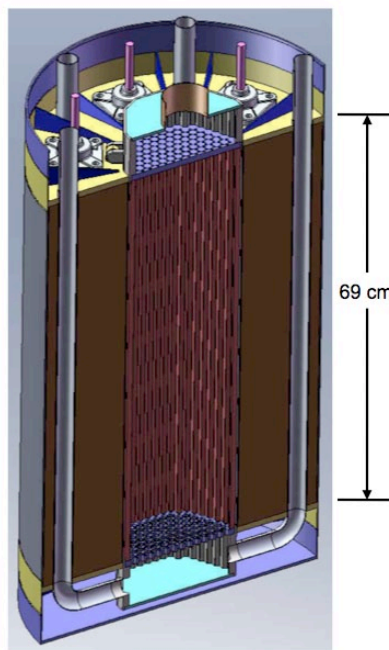


Figure 4-2.—Reactor module axial cut-away view.

### 4.2.1 Fuel Pins

The core contains 163 SS/ $\text{UO}_2$  fuel pins with a 1.28 cm pin OD and a SS-316 clad thickness of 0.051 cm. The fuel meat is assumed to be 94 percent theoretical density, 93 percent enriched  $\text{UO}_2$ , with a nominal 0.0065 cm assembly gap between the fuel and clad (cold/beginning-of-life (BOL)). The cold/BOL height of the fuel column is 48 cm. Within the fuel pin there is 9 cm of BeO pellets at each end of the fuel pellets to serve as an axial reflector. There is a small expansion region at the top of the pin, which also serves as a fission gas plenum; however, the fission gas production/release at this burnup and temperature does not cause stress/creep concerns in the cladding. The operating conditions of the fuel are very benign relative to past reactor experience. The peak fuel burnup is 1.2 percent (FIMA – Fissions per Initial Metal Atom), the peak power density is  $32 \text{ W/cm}^3$ , and the peak linear heat rate is  $3.4 \text{ kW/m}$ . There is no anticipated pellet clad mechanical interaction (PCMI) throughout the life of the reactor because the gap grows with temperature (SS-316 expands at a greater rate than  $\text{UO}_2$ ) and fuel swelling is small ( $\sim 0.8$  percent in the peak pellet). The peak cladding temperature during nominal operation is 860 K (average clad temperature = 828 K). The peak cladding fast fluence is  $5.0 \times 10^{21} \text{ n/cm}^2$ , which is below the threshold of significant ductility loss. The peak center-line (C/L) fuel temperature during nominal operation is 950 K (average fuel C/L temperature is 917 K, overall average fuel temperature is 865 K). A graph showing the average fuel temperature distribution through the core relative to the cladding and coolant temperatures for nominal operating conditions is presented in Figure 4-3.

### 4.2.2 Core Geometry

The reference core uses a triangular pitch pin-lattice arrangement. A tie-structure holds the pins axially and radially on one end, but allows the pins to float axially at the other end. The low power allows pin spacing to be very tight ( $P/D = 1.04$ ), which is beneficial for two reasons: (1) it allows the void fraction to be low enough so that internal safety rods, or other measures, are not needed to maintain flooded subcriticality, and (2) it keeps the potential reactivity effects of pin movements small, even if the spacing mechanisms should fail. Wire wrap is used to help maintain spacing and promote interchannel mixing (although preliminary analysis shows that mixing between channels is not needed in this system). The assembly clearance between the wire and adjacent pin is 0.0076 cm so that ample flow can be provided even if pins are clumped together, and again, to keep reactivity effects small. Flow is highly turbulent ( $Re = 15,000$ ), and the film temperature drop in the coolant is only a few degrees K, so the design is very tolerant of any thermal-hydraulic changes caused by pin movements.

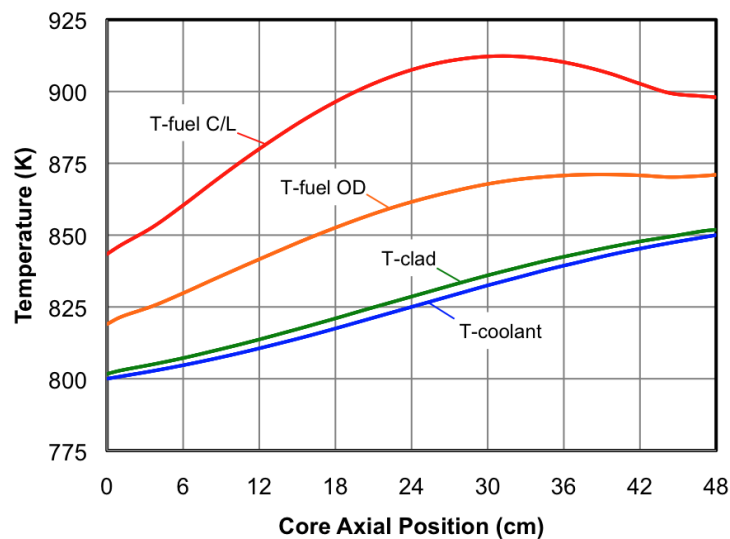


Figure 4-3.—Average core temperature distribution.

### 4.2.3 Vessel and Plenum Geometry

The reactor vessel is 0.25 cm thick SS-316. A dodecahedron vessel is used to allow the radial reflector and control drums to be closer to the fuel, which provides significantly more reactivity swing for postulated accidents (and also reduces mass). The vessel thickness was sized to meet 1/3 ultimate and 2/3 yield stress criteria during the postulated worst-case transient (currently assumed to be unmitigated loss-of-flow). If structural or fabrication issues arise with the dodecahedron vessel, a cylindrical vessel could be used at the cost of reactivity margin and mass. The peak vessel fluence is well below significant SS-316 damage thresholds. There is no coolant downcomer within the reactor vessel. The flow is fed to the bottom plenum of the reactor via piping that travels through the radial reflector (as seen in Figure 4-2). This allows the ex-lattice flow area and hydraulic diameter to be large (minimizing pressure drop), and more importantly brings the radial reflector and control drums closer to the core and removes a potential flooded region in the reactor (making criticality requirements easier to meet). The primary drawback of this approach is that it complicates the core and radial reflector integration (depending on how the shield, reflector, and NaK feed-pipes would integrate in a downcomer design). At the current level of mechanical design, the assembly appears relatively simple for either the pipe-downflow or downcomer configuration, but this feature will depend on more detailed design and analysis.

### 4.2.4 Radial Reflector and Control Drums

The radial reflector is Be metal encased in a SS-316 structure. Be is generally a heavier option than BeO, but Be is less susceptible to radiation/temperature induced swelling and cracking. The Be temperature and fluence in the baseline design is low enough that there should be no significant degradation, and data suggests that swelling will be <1 percent. The radial reflector is 49 cm in diameter, which results in maximum thickness of 15.1-cm (from the smallest vessel flat). The SS-316 can range from 0.1 to 0.2 cm in thickness depending on the location. The control drums are 13.5 cm in diameter, and are composed of Be and a 112° banana-shaped arc of B<sub>4</sub>C absorber, all contained in a stainless steel cylinder. The maximum thickness of the B<sub>4</sub>C within this arc is 1 cm. Each drum is powered by a dedicated motor and drive mechanism to permit angular position changes. A nominal 2-mm radial gap is between the drums and reflector to prevent contact that might impede drum movement. A preliminary thermal-structural analysis performed for the entire radial reflector/drum assembly indicates that there should not be significant bowing or deformation. This analysis shows radial reflector temperatures to be below 800 K; however the peak temperatures in the drums approach 900 K. Further analysis of the current configuration is planned and temperatures could be reduced by a variety of minor design changes if needed.

## 4.3 Heat Transport

The function of the pumped-NaK heat transport system is to deliver reactor power to the Stirling engines. The NaK loops operate at relatively low pressure (~140 kPa) and at temperatures (less than 850 K) for which past experiences suggest corrosion should not be a problem. The major components of the reactor heat transport subsystem are pumps, accumulators, piping, and intermediate heat exchangers (IHXs). Note that the NaK-to-He heat exchanger at the Stirling hot head is considered part of the power conversion system; the reactor heat transport system is assumed to terminate at the NaK pipes that feed the Stirling engines.

The technology required for the heat transport system has been determined; however, the configuration and layout of the flow loop(s) is yet to be finalized. A notional layout of the reactor heat transport system is shown in Figure 4-4 where the primary loop is shown in red and the intermediate loop is shown in green. This arrangement shows a split shield with the intermediate heat exchangers located in-between the shield layers to minimize their contribution to the radiation dose above. Analysis has been performed that indicates this arrangement may not be optimum for the buried configuration, suggesting that the shield could be simplified to a single monolithic structure. However, it still may be prudent to

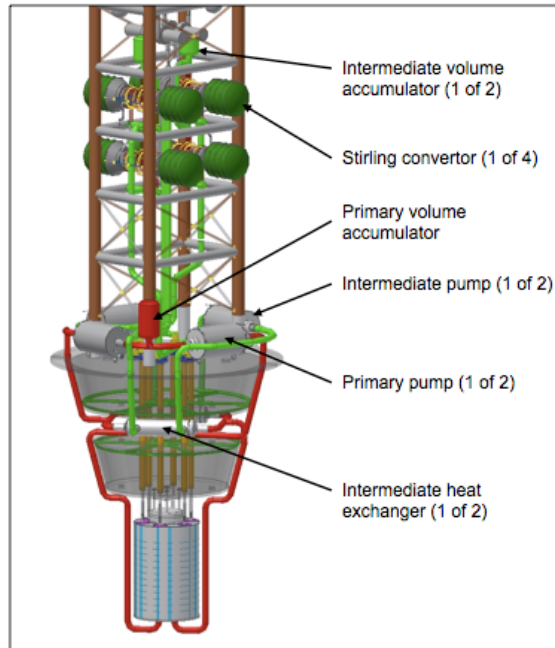


Figure 4-4.—Reactor heat transport layout.

place the intermediate heat exchangers below the stainless steel top-plate of the shield that serves as the primary gamma shield. While this arrangement serves as a good placeholder, the final heat transport configuration will depend on further shielding studies and a more detailed review of the radiation tolerance of equipment located on the truss above the shield.

#### 4.3.1 Number of Loops

One of the key design trades for the FSP system concerns the use of the intermediate heat exchangers (IHX) and flow loops versus direct flow of the primary NaK from the core to the power conversion units. The benefits of the intermediate loop system are: 1) it potentially mitigates the system consequences of a breach of the He-to-NaK interface at the Stirling heater head, 2) it provides a good method to reduce the dose from activated NaK to components above the shield, 3) it allows the temperature drop across the Stirling head to be adjusted and optimized separate from the temperature rise across the core, and 4) it provides more flexibility and a cleaner interface between the reactor and balance-of-plant for the flight unit Assembly, Test, and Launch Operations (ATLO) phase. Some of the disadvantages of the intermediate loop approach are: 1) it adds system complexity by increasing the number of components, 2) it complicates NaK freeze prevention and loop startup including the need for increased startup energy, 3) it adds ~500 kg of mass to the system due mostly to the additional hardware (pumps, accumulators, IHXs), but also because the intermediate loop introduces additional inefficiencies and parasitic losses which increase the required gross system power. For the reference concept, it was decided to include two 50 percent power intermediate loops.

#### 4.3.2 System Flow Configuration

In the notional layout presented in Figure 4-4, the reactor primary loop delivers 186 kWt via heated NaK to a pair of intermediate NaK-to-NaK HXs. The primary loop has a NaK flow rate of 4.3 kg/s, a hot temperature of 850 K, a cold temperature of 800 K, and an estimated loop pressure drop of 20 to 25 kPa (the pressure drop will depend significantly on final loop configuration). The primary NaK coolant flows up the core through the interstitial area between the fuel pins. Flow enters then exits the upper plenum via a single pipe that flows straight through the upper shield. A straight pipe simplifies fabrication and integration, and radiation streaming is not a problem given the current configuration and shield requirements because the solid angle of a 1-mm gap is very small over a 1-m run of piping. The primary

flow then splits into two 50 percent flow pipes and passes in parallel through the tube side of the tube-and-shell IHX. The flow then recombines into a 100 percent flow pipe and passes through the two primary pumps in series. After a pass by the accumulator, which is connected to the loop by a tee, the flow then splits into six smaller pipes that travel back down through the shield. These pipes then reduce in size and continue straight through the radial reflector, below which they bend inward to feed the reactor lower plenum. While straight pipes simplify fabrication and integration, they can also exacerbate thermal expansion/stress issues in the flow loop. If expansion stresses make mechanical design problematic for the flight system, more stress relief features will have to be incorporated into later loop designs.

Each intermediate loop delivers 93 kWt via the heated NaK to two Stirling convertors arranged in parallel. The intermediate loops have a NaK flow rate of 3.5 kg/s, a hot temperature of 824 K, a cold temperature of 794 K, and an estimated loop pressure drop of 9 to 12 kPa. The intermediate NaK flow proceeds from the shell side of the IHX, splits into two 50 percent flow pipes and proceeds to the two Stirling convertors (technically each Stirling convertor is a pair of opposed Stirling engines, but functionally they serve as a single unit). The flow passes across the Stirling heater heads, recombines into a full flow pipe, passes by the intermediate volume accumulator, enters the intermediate loop pump, and returns to the shell side inlet of the IHX.

### 4.3.3 NaK Pumps

There are a total of four NaK pumps in the reference system: two pumps in the primary loop (each capable of 100 percent flow for redundancy), and one pump in each intermediate loop. The reference approach is to use separate, optimized pump designs for the primary and intermediate loops. These pumps would be optimized in size and performance, but would share the same technology basis.

The FSP NaK pump is based on Annular Linear Induction Pump (ALIP) technology. The design concept is shown in Figure 4-5. The pump consists of a series of magnetic coils surrounding a cylindrical duct with an internal torpedo to increase fluid velocity. It operates on three-phase power with three circuits containing four coil sets each. The pump duct has no moving parts and no direct electrical connections to the wetted NaK components. Pressure head is developed by the interaction of the magnetic field produced by the stator and the electrical current that flows in the liquid metal as a result of the induced voltage. Flow can be controlled by varying the frequency and/or the voltage supplied to the pump windings. The FSP primary pump is designed for a nominal frequency of 36 Hz and a nominal supply voltage of 72 V. This ALIP is designed to supply a maximum pressure head of 69 kPa to liquid NaK flowing at 4.3 kg/s with an adiabatic efficiency of 15 percent at nominal flow conditions. The intermediate loop pump is of similar design with about one-half the developed pressure head and a nominal NaK flow rate of 3.5 kg/s.

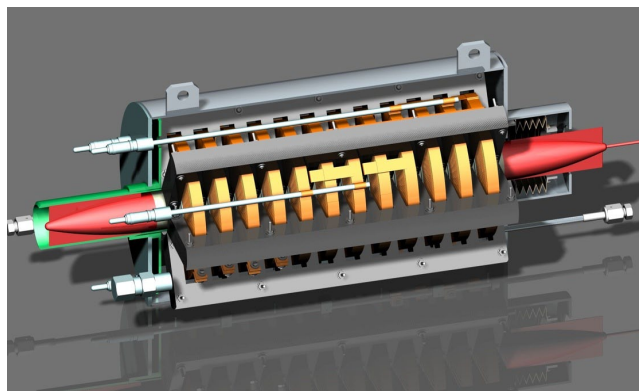


Figure 4-5.—Annular linear induction pump.

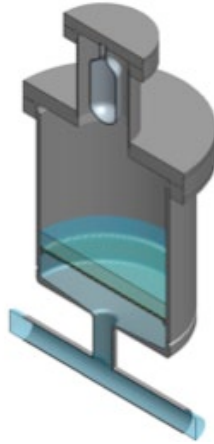


Figure 4-6.—NaK volume accumulator.

TABLE 4-4.—PRIMARY LOOP VOLUMES AND PRESSURES AT VARIOUS CONDITIONS

Loop parameter	Minimum temperature	Room temperature	Operation temperature	Maximum temperature
Ave. coolant temperature, K	264	295	810	1000
NaK density, g/cm <sup>3</sup>	0.88	0.87	0.75	0.70
Vapor pressure, kPa	0.0	0.0	5.4	56.6
Loop physical volume, L	49.9	50.0	51.4	52.0
Total NaK volume, L	57.6	58.1	68.2	85.1
Total physical volume, L	105.6	105.8	108.8	110.1
Gas volume, L	48.0	47.7	40.6	25.0
Gas pressure, kPa	34.5	38.8	125.1	250.9
Total pressure, kPa	34.5	38.8	130.4	307.5

#### 4.3.4 Volume Accumulators

There are three accumulators in the FSP reference system, one for the primary loop and one for each of the two intermediate loops. The FSP reference uses fixed-volume accumulators for the flight system, as shown in Figure 4-6, rather than a bellows-type system. An initial charge of inert gas sets the pressure of the system, and thereafter determines the loop pressure as a function of NaK and gas temperature. In a simple free-surface system, positioning of the volume accumulator at the highest point of the system is desirable to ensure proper gas/liquid separation. However, the uncertainties in orientation and gravity-loading that occur during ground handling, launch, and delivery may necessitate the use of mesh screens to maintain gas within the accumulator volume. Mesh screens could be very beneficial in microgravity type conditions, but additional study is required to verify if the combination of the high NaK surface tension and 1/6-g on the Moon will provide adequate free-surface behavior in conjunction with a screen. Future analysis and testing will be performed to assure that gas can be retained in the accumulator volume under all credible scenarios, and whether a simple free-surface system is sufficient or a mesh-screen is necessary to properly contain gas. The potential also exists to utilize multiple accumulator volumes at various locations in the system to reduce the sensitivity to orientation and gravity.

Four parameters were used to size the reference case primary loop accumulator: room temperature loop volume (50 liters), accumulator cold coolant volume (8 liters), accumulator peak gas volume (25 liters), and gas pressure at cold conditions (34.5 kPa or about 5 psi). These conditions result in a primary accumulator with a total room temperature volume of 56 liters and 0.76 moles of fill gas. The change in loop volumes and pressures at various state points is shown in Table 4-4. A similar process was used to size the intermediate loop accumulators.

The maximum design-basis loop temperature has not been determined, but a value of 1000 K may be a reasonable limit. In an over-temperature transient the loop pressure will depend greatly on the difference between the average coolant temperature and the accumulator gas temperature (in the above table, it is conservatively assumed that the coolant and gas temperature are the same). The values in

Table 4-4 are at beginning-of-life, and pressures will increase slightly throughout lifetime as gases are produced due to neutron capture in the NaK. The total gas production over the 8-year life at full power has been calculated as approximately 0.05 moles: 0.01 moles of He and 0.04 moles of Ar. There are also 0.5 moles of H produced, but it is presumed to leak out of the system through the stainless steel containment due to high hydrogen permeation in stainless steels at these temperatures. The gas production is predicted to increase primary loop pressure by 7 percent over the 8 year system lifetime.

#### 4.3.5 Heat Exchangers

The FSP reference concept includes two IHXs. The reference is to use a standard one-pass tube-and-shell configuration as shown in Figure 4-7. In order to minimize radiation and provide some protection against primary loop fluid leaks, the preferred configuration has the primary flow through the tubes and the intermediate flow through the shell. There is considerable experience with small liquid-metal-to-liquid-metal tube-and-shell heat exchangers; therefore this component is not viewed as a significant technical risk to the program. However, this IHX may have to be more robust internally than traditional heat exchangers. In many tube-and-shell designs, it is generally accepted that internal leaks may occur between the tube and shell side, and the only penalty is a small drop in effectiveness. For FSP, as was discussed above, an important reason for selecting the intermediate loop option was to mitigate a He-to-NaK breach from propagating to the primary loop. A possible mitigation approach is to fully contain the helium leak in the intermediate loop volume should a breach occur at the Stirling heater head interface. It has been determined that it would be impractical to oversize the intermediate volume accumulators to accommodate the Stirling gas volume. Thus, either the intermediate-side of the IHX NaK containment boundaries would have to survive the pressure surge, or some form of pressure relief in the intermediate loop would be required. The current FSP technology program includes fabrication and testing of a flight-like IHX.

#### 4.3.6 Other Components

The FSP flow loops may or may not have chemistry control (e.g., cold traps). Previous experience with stainless steel and NaK loops has indicated that corrosion should not be a problem as long as the initial fill of NaK is very low in oxygen content (<20 ppm). Multi-foil insulation will likely be used on the heat transport system and all high temperature surfaces. In general, the loop will be insulated as much as possible; however, there is a benefit to have some heat loss in the flow loop to mitigate the consequences of certain thermal transients.

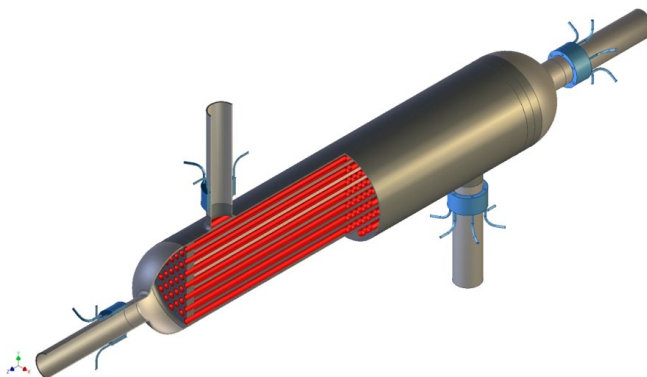


Figure 4-7.—Intermediate heat exchanger concept.

## 4.4 Instrumentation and Control

The functions of the Instrumentation and Control (I&C) subsystem are broadly categorized as measurement, monitoring, communication, and control. The nature and interrelationship of these functions define the overall architecture. The method of communicating with the FSP system is not yet defined; it will likely include some local monitoring at the outpost as well as data telemetry back to Earth. System startup is the operational phase most dependent on interactive communications and it is desirable to have near real-time sensor data returned to Earth when the reactor is being started. Data rates and the number of reported parameters can be reduced once the system has reached steady-state operation.

After installation, the reactor is started using a limited supply of auxiliary electric power to operate the NaK pumps and move the reactivity control drums. The startup sequence can be performed with human assistance by issuing commands from an Earth-based control station using high data-rate communications. Alternatively, the startup could be performed locally by trained astronauts with support from Earth-based operators. Preprogrammed sequences with frequent hold-points are currently envisioned for the startup sequence. The approach is similar to control schemes developed and used on the Mars Exploration Rovers (MER) Spirit and Opportunity, in which the drive system is commanded from Earth and measured steps are taken with time allocated for operators to examine progress before deciding on subsequent steps. If communications are lost during FSP startup, the reactor may need to automatically respond to unanticipated events and therefore some level of autonomy is anticipated. If communications are lost to the FSP system during normal operation, the system can continue to operate without interruption.

The reactor has a very limited number of control parameters and only two controllable hardware elements: the NaK pumps and the control drive motors. The voltage and frequency of the electrical power supplied to the pumps are control variables that could be adjusted during the startup phase of operation. Once system equilibrium has been achieved, the pump power will be essentially fixed, which will maintain a constant flow rate in the three coolant loops. Prior to system startup, the pumps may be periodically exercised to circulate the NaK to prevent freezing.

The six rotating drums contain neutron-reflecting (Be) and neutron-absorbing ( $B_4C$ ) materials. To increase the reactivity of the system the drums are rotated so that the beryllium is facing the core and the  $B_4C$  is facing away. The six drums are independently moved by dc stepper motors and are grouped into two categories. Three of the drums are “startup” drums. Startup drums rotate faster than the other three drums and are simultaneously rotated to the most reactive position prior to the ascent to power. The reactor system will remain subcritical with the startup drums in this operating position. The remaining drums are “fine-control” drums. The fine-control drums rotate slower than the startup drums and need not fully rotate to cause the reactor to become critical. Also they do not have to fully rotate for the reactor to function during the planned service life. The use of six drums for reactivity control provides redundancy to allow the system to complete the mission if one of the drums fails to move from the least reactive position. The control drums therefore have excess reactivity and the control system must carefully maintain drum position to avoid inserting more reactivity than desired. If two drums fail to move from the least reactive position then the system cannot produce power.

A notional control drum drive gear assembly is shown in Figure 4-8. The assemblies mount to the top plate of the axial reactor shield. Connecting rods penetrate through the axial shield to attach the drives to the top of the control drums. This is a fairly high radiation region but commercial motors and dry-lube gear assemblies have been identified that appear suitable for this environment. Independent stepper motors rotate each gear assembly to engage a connecting rod and rotate a drum. Fine-control drums may have a different gear ratio than startup drums but otherwise the control drum drive assemblies are identical. The startup drums are normally in their most reactive position and any rotation of these drums can only reduce the reactivity of the system. Allowing all three startup drums to operate simultaneously while precluding the motion of more than one fine-control drum assures that negative reactivity insertions are faster than positive ones. Thus the startup control drums also serve an important safety function.

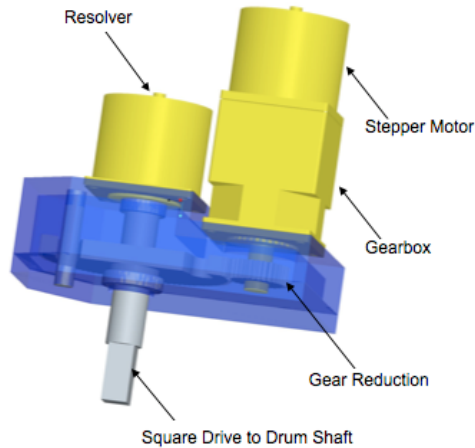


Figure 4-8.—Control drive motor assembly.

TABLE 4-5.—PRELIMINARY REACTOR SENSOR LIST

Sensor/measurement	Count
Thermocouple	52
Resistive Thermal Device (RTD)	8
Pressure transducer	6
Position encoder	12
Flow rate	6
Neutron detector	4
Gamma detector	2

During normal steady-state full power operation the reactivity of the system will gradually decline due to fuel burn-up and small reactivity insertions using the three fine-control drums will be required periodically to maintain the reactor temperature within a reasonable band. The reactor does not require frequent reactivity control action and can operate without control drive power for extended periods with the only consequence being a small and gradual reduction in the reactor coolant outlet temperature and system electrical output. The FSP system can continue to safely produce power for months (and perhaps much longer) without any reactivity adjustment, as was demonstrated with the SNAP-10A ground test reactor, which operated for more than 10,000 hr without reactivity adjustment.

The system will be designed to safely ride-out transients associated with normal operation (i.e., changes in environmental conditions related to sunrise and sunset) and respond promptly to sudden unanticipated events if required. It is expected that the system will be able to tolerate most credible component failures without requiring an active control system response. The inherent negative-temperature reactivity feedback of the reactor should be sufficient for responding to possible failure modes such as the loss of a primary pump (invoking the need to switch to the backup pump) or the loss of a single Stirling convertor. However, some control action may be desired to mitigate the transient effects on the core structure, components, and materials. The required response to more severe events such as an extended stoppage of reactor coolant flow or a loss of the coolant inventory will be evaluated in more detail as the system design evolves.

The sensors to measure system performance parameters are dispersed mainly on the flow loops and power conversion units above the axial shield and are generally not very sensitive to radiation. A summary of the reactor sensors is provided in Table 4-5. Radiation sensitive electronics to amplify the signals from the sensors and to control the drive motors are located in protective enclosures near the top of the radiator support truss where the radiation fields are much lower. Separate enclosures are envisioned to provide physical redundancy for all essential components and standard multiple-redundant command and control schemes will be used to manage the system. The boxes may be heated to protect components

from the extreme cold on the surface during the lunar night. The enclosures also provide radiation protection for the electronics. Current estimates indicate that electronics commonly used in the aerospace and satellite industry can be used for the reactor I&C because the radiation doses above the shield in the buried configuration are relatively low.

## 4.5 Radiation Shield

There are two primary aspects to designing a radiation shield for the FSP reactor: 1) radiation dose to the FSP components, and 2) radiation dose to astronauts located at the outpost or other locations where they would spend a significant length of time. The radiation limit to FSP components is currently set at less than 5 Mrad (gamma) and  $2.5 \times 10^{14}$  nvt (neutrons). The radiation limit to a crew member from the FSP system is currently set at less than 5 rem per year. The shielding of the astronauts is highly dependent on the FSP installation approach, e.g., reactor buried in regolith, placed on the surface, or left on the lander. The shielding required for the local FSP components is less dependent on the installation since the basic FSP configuration is largely fixed (i.e., a vertical arrangement with the reactor at the bottom and the non-nuclear components on a truss above with an axial shadow shield between the two). However, a buried reactor can significantly decrease the dose to the above-surface components because the surrounding regolith serves to reduce radial neutron leakage. The resulting dose to FSP components from radial leakage would be greater for a surface-mounted or lander-integrated FSP system.

The reference approach for the FSP system assumes the buried configuration. The radiation analysis of the buried reactor is fairly sensitive to hole geometry and regolith properties (e.g., density, thermal conductivity, and composition). There are several possibilities for the geometry of the hole such as a trench, slot, or cylinder. The reference concept assumes that the reactor is placed in an oversized cylinder that is backfilled with regolith. This is a more conservative approach for below-grade shielding because the reactor is fully surrounded by a lower density backfill (assumed to be  $1.4 \text{ g/cm}^3$ ) as opposed to undisturbed regolith (assumed to be  $1.8 \text{ g/cm}^3$ ). The significance of the lower density regolith is that it allows more neutrons to leak to the surface, which can scatter or produce secondary-gammas that reach the outpost or local FSP components.

A layout of the buried reactor shield configuration is shown in Figure 4-9. The reference shielding material is  $\text{B}_4\text{C}$  powder enriched to 90 percent  $^{10}\text{B}$  with a packing fraction of 75 percent.  $\text{B}_4\text{C}$  was selected over water for this configuration because of the demanding thermal environment and the more straightforward development. Water shielding may be preferred for above-surface reactor installations due to the mass benefits. For the buried reactor, the mass benefit of water shielding is diminished because of the need for gamma shielding to prevent overheating of the regolith. Boron carbide is a well-established nuclear material, as it has been utilized extensively as a neutron absorber (for control and shielding) in the majority of terrestrial reactors. One drawback to the  $\text{B}_4\text{C}$  powder is the very low thermal conductivity, particularly in vacuum. The concern is not necessarily that the  $\text{B}_4\text{C}$  will overheat, but rather the difficulty of transferring reactor power losses through  $\text{B}_4\text{C}$  to external heat pipes that reject the waste heat above the surface. This power deposition is particularly challenging for off-nominal transients (e.g., loss of reactor cooling). The proposed solution is to put a large number of stainless steel ribs within the shield to help conduct the power losses. The use of curved ribs serves to impede gamma streaming and reduce the required gamma shield mass. As shown in Figure 4-9, the axial shield has an open cavity in the region directly above the reactor. MCNP analyses indicate that placing  $\text{B}_4\text{C}$  in this volume does not measurably reduce the dose above the surface. This cavity void has the combined benefit of reducing the mass of  $\text{B}_4\text{C}$  and simplifying the thermal management since the power losses can be distributed over a larger surface area and the through-thickness conduction path can be reduced. The truncated cone section at the top of the shield helps to decrease scattered radiation from the regolith to components located on the truss.

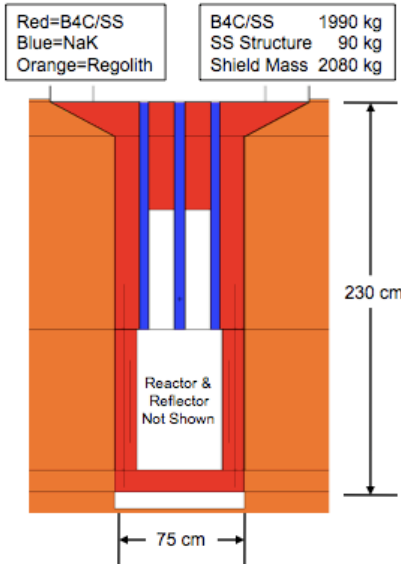


Figure 4-9.—Buried shield layout.

Early concepts did not include the lower section of B<sub>4</sub>C shielding around the core, which resulted in much lower shield mass. However, an analysis of the system thermal balance found that the local regolith temperatures could become problematic due to the regolith's poor conductivity. The amount of neutron and gamma fission power that is deposited into the regolith was estimated at more than 2 kWt. A heat conduction model, using the conductivity of loose regolith, calculated peak temperatures above the melting temperature of regolith. It is possible that the regolith will sinter, and thus increase the conductivity to a level where overheating would no longer occur, but this may be hard to verify prior to operation on the Moon. Further, the sintered material might crack and leave radiation streaming paths to the surface. The heated regolith might also out-gas materials that could damage the FSP system. To avoid these possible issues, the reference buried case utilizes a radial shield that reduces the regolith power deposition by an order of magnitude; thus maintaining the peak regolith temperature at approximately 1000 K. In total, the radial and bottom shields add about 1000 kg to the system including about 500 kg of stainless steel. If higher regolith temperatures are permitted, the mass of the lower shield could be decreased or it could be eliminated altogether.

#### 4.6 Reactor Thermal Control

An important aspect of the FSP reactor design process is to ensure that component temperatures are within acceptable limits during normal operations and during possible fault scenarios where overheating or overcooling may occur. Approximately 3 to 4 percent of fission power is deposited in the radial reflector and shield (~2 percent radial reflector, and ~1 to 2 percent in the shield depending on the installation approach). This power, plus a small fraction of thermal radiation from the vessel to the radial reflector, must be rejected from the external system boundary during normal operation. A summary of ex-core power deposition is presented in Table 4-6.

Figure 4-10 contains a contour plot of the system power density (W/cm<sup>3</sup>) in the x-y and x-z planes. Most of the power is in the fuel, which is easily discernable by the bright red colors on the plot. In contrast, any location that is void of material is deep blue because there is no power deposition in a vacuum; the voids of the fission gas plena can be seen in the x-z plot just below the upper NaK coolant plenum. Note that the NaK regions are lighter than others because of the low density material and low cross-sections.

TABLE 4-6.—REACTOR MODULE POWER LOSSES

Region	Power, W
Radial reflector Be	924
Radial reflector SS	121
Drum Be	1376
Drum SS	256
Drum B <sub>4</sub> C	1190
Total in radial reflector	3867
Upper shield	210
Radial shield	2265
Lower shield	356
Total within cavity	6698
Regolith	194
Total outside of core	6892

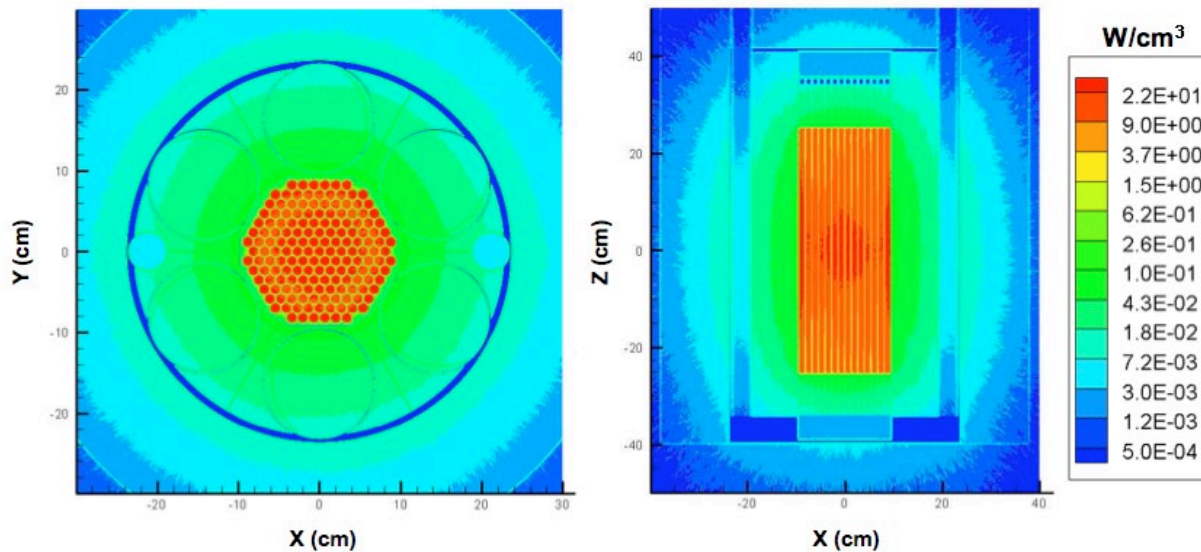


Figure 4-10.—Reactor power density contours.

As was discussed earlier, it is desirable to maintain beryllium temperatures within the range between 750 and 800 K during nominal operation. This proves to be difficult if simple thermal radiation gaps are assumed between components and materials within the components. Potentially more difficult than steady-state thermal balance is the removal of decay heat during transients that reduce coolant flow and fission power to near-zero. During loss-of-power conversion load or loss-of-flow transients, more power is radiated from the vessel to the radial reflector, but there is a substantial drop in fission power deposition; thus the total power rejected from the system decreases.

One of the challenges of an emplaced system is heat removal from ex-core components and core decay power during certain transients, as well as protection of equipment from regolith interactions and/or infiltration. Since regolith is a very poor thermal conductor, the reference design includes a shroud surrounding the reactor assembly that is cooled by H<sub>2</sub>O heat pipes coupled to a small radiator above the surface. This shroud is integrated with the outside of the shield and extends above to provide a regolith boundary for the components on the top face of the shield. Thermal balance and transient calculations have estimated that a nominal radiator temperature of 370 K is required. The peak power rejection of this system would be between 5 and 7 kWt, depending mostly on the amount of core radial shielding. One additional advantage of a H<sub>2</sub>O heat pipe rejection system is that the heat pipes will stop transferring heat

below a certain threshold temperature. This will significantly decrease heat removal from the reactor assembly at low operating temperatures because of the insulating effect of the regolith.

The reference design approach is to keep the reactor NaK molten at all times, avoiding the need to accommodate freeze/thaw cycles. If the reactor has been operated and shutdown, decay heat should be sufficient to assure that the coolant remains liquid for some time. Prior to operation, calculations have shown that the bulk NaK will not freeze during a 354 hr lunar night, assuming standard multi-foil insulation on all exposed surfaces. As a contingency, trace heating could be added to the NaK piping, and the pumps could be occasionally exercised at low power to circulate and heat the fluid. During the lunar day, the higher environmental sink temperature due to solar heating should preclude any possibility of NaK freezing.

## **5.0 Balance-of-Plant (BOP)**

The FSP BOP includes the power conversion, heat rejection, and PMAD modules. In general, the design responsibility for the BOP is assigned to NASA while the design responsibility for the reactor module rests with DOE. In practice, there is an integrated design process in which both sides contribute in defining the overall system concept. Most of the key design decisions on the BOP concern heat and electrical interfaces to the power conversion module. How does the reactor heat get in? How does the waste heat get out? How does the electric power get to the users?

### **5.1 Key Balance-of-Plant Design Decisions**

#### **5.1.1 Power Conversion Technology**

As mentioned previously, the FSP reference concept selection process (Section 1.2) included studies of four different power conversion technologies with the liquid-metal reactor heat source: 1) Stirling, 2) Brayton, 3) Rankine, and 4) thermoelectric. The analyses performed during the reference concept selection indicated a clear performance advantage for Stirling power conversion given the 900 K heat source temperature assumption and the 40 kWe output power requirement.

Figure 5-1 shows a comparison of relative reactor thermal power (inversely proportional to efficiency), radiator area, and system mass among the four power conversion options assuming a UO<sub>2</sub> fueled, fast-spectrum, NaK-cooled reactor heat source with a maximum coolant temperature of 900 K. The liquid-metal (LM) Stirling option is based on the FSP preliminary reference concept: single NaK primary loop, two NaK intermediate loops, four free-piston Stirling power conversion units (PCU) with He working fluid, four H<sub>2</sub>O heat rejection loops, and composite radiator panels with Ti/H<sub>2</sub>O heat pipes. The LM-Brayton option assumed a primary NaK-to-CO<sub>2</sub> reactor interface, two closed Brayton PCUs with CO<sub>2</sub> working fluid, H<sub>2</sub>O heat rejection, and composite radiators with Ti/H<sub>2</sub>O heat pipes. A LM-Brayton alternative with HeXe working fluid was also evaluated and found to have lower performance than the CO<sub>2</sub> version. The LM-Rankine option assumed a primary NaK-to-toluene reactor interface, two organic Rankine PCUs with toluene working fluid, H<sub>2</sub>O heat rejection, and composite radiators with Ti/H<sub>2</sub>O heat pipes. The use of toluene limited the reactor supply temperature to 750 K to preclude thermally-induced decomposition. The LM-thermoelectric (TE) option assumed four primary NaK heat exchangers with integral PbTe/TAGS TE modules, NaK heat rejection, and composite radiator panels with SS/K heat pipes.

As shown in the graph, the reference LM-Stirling approach offers the lowest reactor power, radiator area, and system mass among the options. The Brayton concept requires a 30 percent increase in reactor power and almost twice the radiator size, while the Rankine approach requires 40 percent more reactor power and 60 percent greater radiator area. The thermoelectric option requires almost 5X the reactor thermal power and over twice the radiator area.

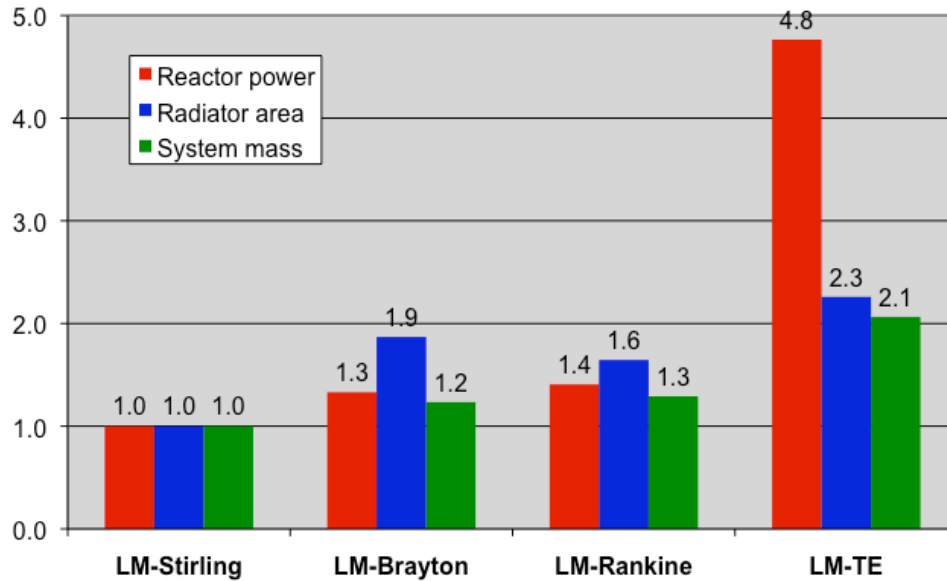


Figure 5-1.—Relative performance of various power conversion options.

There are additional factors beyond performance that must be considered in selecting a power conversion approach, particularly technology readiness. A technology assessment and relative cost evaluation by the FSP team led to the conclusion that the LM-Stirling concept could meet the project affordability goals with reasonable development risk. Brayton conversion was selected as a potential back-up should development issues arise with the Stirling option.

### 5.1.2 Converter Size and Number

The goal to produce partial power in the event of unexpected failures led to a decision to use redundant power conversion units. Partial power operation of the FSP system should be sufficient to meet essential crew power requirements (e.g., life support). It may also be desirable to operate at partial power during extended periods of inactivity. In general, fewer conversion units result in lower system mass due to the convertor's economy-of-scale with increasing power and the reduced amount of interface plumbing. More units generally improve system reliability because of the increased fault tolerance, although there is a limit since greater part count can also increase complexity and failure potential. An objective in developing the FSP reference concept was to use the minimum number of power conversion units to achieve adequate system redundancy while not exceeding a reasonable unit power size.

In the 1980's, a 25 kW dual-opposed free-piston Stirling convertor was developed for SP-100 reactor applications. While this development activity was generally considered successful, the corporate infrastructure to design and manufacture this class of Stirling convertor is not readily available today. Conversely, today's free-piston Stirling manufacturers are focused on 100 W-class Stirling convertors to support Radioisotope Power System (RPS) applications. In addition, the terrestrial power market has led to the development of commercial kilowatt-class Stirling machines for residential co-generation and small dish-electric systems. The RPS and commercial Stirling markets provide a better starting point for FSP technology than the 1980's Stirling designs. The FSP team believes that this technology can be leveraged to achieve 10 kW-class convertors without introducing excessive development cost and risk. Further, limiting the design to this power level allows the Stirling heater head to retain a relatively simple and conservative monolithic heater head arrangement avoiding the need to develop complex acceptor heat exchanger geometries for the pumped-NaK heat source. The FSP reference concept uses four dual-opposed 12 kW Stirling convertors. This approach provides a practical convertor size and reasonable system fault tolerance.

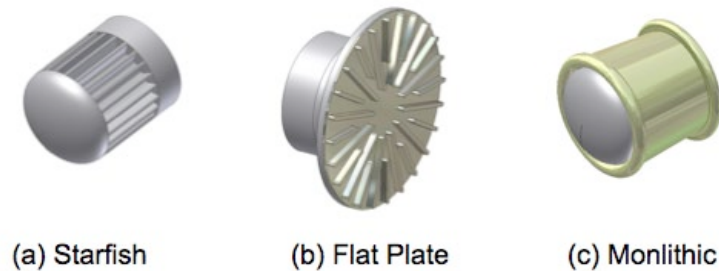


Figure 5-2.—Stirling hot-side heat exchanger options.

### 5.1.3 Power Conversion Heat Input

Several options were considered in the physical design of the reactor-to-Stirling heat transfer interface. The Stirling heat acceptor is typically an annular section of helium flow passages around the displacer cylinder inside the Stirling pressure vessel. The geometry is generally constrained by Stirling thermodynamic performance to be relatively small in diameter with a short axial length. This makes the heat source interface somewhat difficult because of the limited area available for heat transfer. It is further complicated by the need to transfer the heat through the Stirling pressure vessel wall, which must have adequate thickness to contain the high-pressure helium working fluid.

Some possible Stirling hot-side heat exchanger options are shown in Figure 5-2. Previous Stirling concepts with liquid metal reactors, such as SP-100, used a “Starfish” heater head in which the pumped liquid metal passed over an extended sodium heat pipe surface containing many small helium flow channels. One could also develop a “Starfish” arrangement with direct coupling to the pumped liquid metal via radial fins containing the helium flow channels. Another option is to use an extended helium surface that results in a flat plate heat transfer interface on the end of the Stirling dome. Both of these options are particularly attractive as engine power levels increase since they extend the Stirling acceptor heat transfer surface area to simplify integration. However, both options also introduce greater complexity for the Stirling helium pressure boundary due to the larger number of helium joints. This makes the manufacturing process more difficult and potentially increases the probability of helium containment failure.

The reference FSP concept approach to the Stirling heat input is an annular NaK flow jacket surrounding a monolithic heater head. This is the simplest and most straightforward method. The jacket would include toroidal manifolds at the inlet and outlet. For the dual-opposed engine configuration, a single jacket could extend over both heat acceptors with a common NaK space between the domes. If desired, the NaK could be fully contained in a SS316 sleeve with a thin SS316 wall between the NaK and the Stirling pressure vessel. This might allow the use of an alternate material for the Stirling head such as Inconel 718 or Mar M 247 without introducing new materials into the NaK containment boundary. A variant on this approach is to move the Stirling pressure containment outside of the NaK annulus to minimize the heat transfer wall thickness. In all cases the helium would flow through an internal fin structure that is closely coupled to the NaK boundary. The ability to use the monolithic head and annular NaK flow jacket is the result of limiting the Stirling unit power size and the corresponding NaK heat flux. As mentioned earlier, this provides the combined benefit of a relatively low-risk unit power scale-up and simple heat exchanger construction.

### 5.1.4 Power Transmission

Lunar and Mars FSP systems are likely to be remotely located from the habitat area and user loads in order to provide suitable separation between the crew and the reactor. Installing the reactor in a pre-excavated hole allows for minimum separation distances since the regolith provides an excellent radiation shield. Nevertheless, long distance power transmission is an expected requirement for FSP.

The reference concept assumes that the Stirling generator output is directly transmitted to the FSP electronics that are located 100 m from the reactor at the outpost. It is desirable to locate the electronics with the crew to allow easy connection of power loads and easy access should electrical maintenance be required. By locating the electronics away from the reactor, it also allows the PMAD to use standard space-rated components rather than more costly radiation-hardened electrical parts. This architecture is enabled because the Stirling generators can produce relatively high voltage, thus avoiding large power cable mass penalties. The baseline assumption is that the Stirling generators produce 400 Vac rms at full power. This is well within the established technology base for permanent magnet linear alternators. The 400 Vac transmission also permits the use of commercially available 600 Vdc-rated electronics and switches. The direct transmission approach would be applicable for power levels up to about 50 kWe and transmission distances up to about 500 m. Beyond 500 m, a higher voltage alternator or a Stirling step-up transformer may be used to achieve reasonable power cable mass values.

### **5.1.5 Power Conversion Cooling**

The reference concept Stirling cold-end temperature is approximately 425 K. This temperature is roughly based on a system mass optimization. For a fixed hot-end temperature, lower cold-end temperatures lead to higher efficiency and less reactor thermal power, while higher cold-end temperatures lead to smaller radiators. The Stirling cold-end temperature is generally determined by balancing the reactor heat source (and shield) mass with the heat rejection mass. Cold-end temperatures much lower than 425 K make it problematic to reject the waste heat during lunar daylight conditions when the sink temperature is greatest.

The 425 K cold-end defines the operating temperature of the heat rejection module. Options for cooling the power conversion units include single-phase pumped-loops or heat pipes. The large FSP heat rejection load and relatively small Stirling heat transfer interface generally leads to a pumped-loop solution, especially considering the distributed nature of the radiator panels. The operating temperature is somewhat low for liquid metal coolants and somewhat high for conventional fluorocarbon and hydrocarbon coolants. Further, the fluorocarbon and hydrocarbon coolants may not be practical for use near the reactor due to the radiation environment. Single-phase water coolant was selected for the reference concept. Water provides an excellent heat transfer fluid with very high specific heat to minimize the required flow rate and pump power. A pumped water cooling system can be developed using near-term technology with relevant flight heritage for pumps, heat exchangers, and accumulators (e.g., International Space Station). The main drawbacks to water are the high operating pressure (saturation pressure at 425 K is about 0.5 MPa or 73 psia) and the volume expansion that occurs with freezing. The high pressure can be accommodated with high strength containment materials and increased pipe wall thickness.

The planned water loop material is titanium. Titanium and water are very compatible with no long-term chemistry or corrosion issues, and this has been corroborated by long-term life testing of titanium-water heat pipes at GRC. Further, titanium is sufficiently strong to contain high-pressure water using commercially-available pipe wall thicknesses (e.g., 0.035 or 0.065 in.). Titanium joining for titanium water fluid systems is also fairly mature.

Water freezing and volume expansion are also partially addressed through the high strength titanium containment. There are other coolants that offer lower freezing temperature, but they do not offer the same thermal-hydraulic properties as water at the planned heat rejection operating temperatures. The current plan is to store the water in heated tanks prior to startup to avoid freezing, and then charge the cooling loops just prior to initiating reactor heatup. The thermal shock and potential flash freeze caused by introducing warm water to a cold radiator duct could be alleviated through the use of strip heaters on the manifold and/or solar heating on the radiator surface. During operations, the use of two parallel water loops on each radiator wing ensures that if one loop becomes stagnant or frozen, the other loop can be used for thawing if necessary. This functionality has been recently demonstrated in radiator testing at GRC.

### 5.1.6 Radiator Technology

The radiator panels are the most visible feature of the FSP system, but not the most massive. The use of lightweight composite materials allows the panels to be easily suspended from the center truss. The radiators must be compatible with the power conversion rejection temperature and water cooling loop, tolerant to the lunar environment and reactor-induced radiation environment, and stowable so that the FSP system can be easily packaged in the lunar lander payload envelope.

The state-of-the-art in large space radiator technology is the International Space Station (ISS) Heat Rejection System (or similar Photovoltaic Radiator). The ISS HRS is a deployable, pumped-ammonia radiator assembly with aluminum facesheets, aluminum honeycomb, and stainless-steel flow channels. The ISS HRS includes eight radiator panels measuring 2.7 by 3.4 m each that extend to a deployed length of 23 m using a motor-driven scissor mechanism as shown in Figure 5-3. The total ISS HRS mass is 1123 kg and the total two-sided deployed area is 147 m<sup>2</sup> for an effective areal mass of 7.6 kg/m<sup>2</sup>.

The use of composite materials can reduce the heat rejection system areal mass relative to the ISS design by as much as 50 percent. Composite materials have become more prevalent in space radiator applications because of their low mass, high thermal conductivity, and high strength. The reference FSP radiators utilize polymer matrix composite facesheets with graphite fibers and epoxy resin. This combination offers excellent thermal-structural properties, good temperature margin, low out-gassing, and radiation resistance in an assortment of commercially available products. The composite facesheets form a sandwich around a series of regular-spaced circular heat pipes contained in square graphite saddles as shown in Figure 5-4. The space between heat pipes may be empty or filled with a lightweight graphite or honeycomb structure. The need for filler material will depend on launch and landing load requirements, which are not known at this time. The use of embedded heat pipes is preferred for the FSP radiator application to provide redundancy and fault tolerance against micrometeoroid impacts. If a heat pipe were to fail or be damaged by micrometeoroids, the adjacent heat pipes could readily assume the heat load without a major effect on system performance.

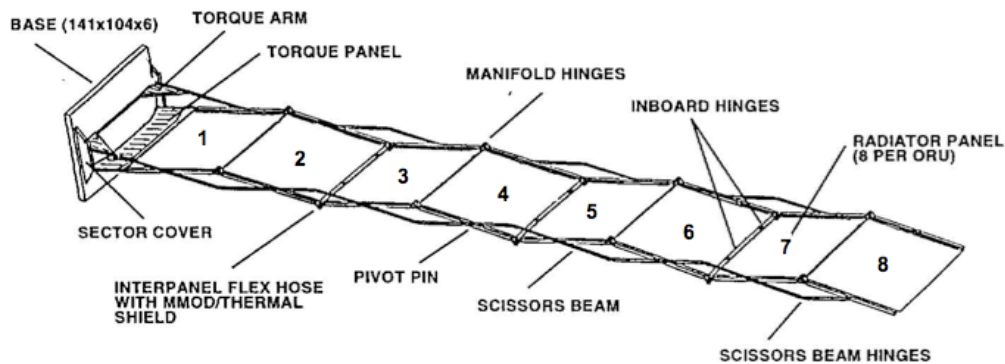


Figure 5-3.—International Space Station heat rejection system.

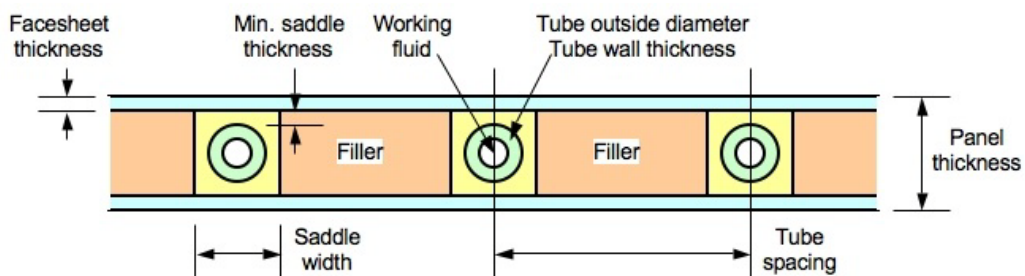


Figure 5-4.—Radiator panel cross-section.

The FSP radiator subsystem utilizes two-sided vertical radiator panels. The maximum sink temperature at the lunar equator for a vertical radiator is approximately 320 K whereas the maximum sink temperature for a horizontal radiator would be about 275 K (assuming a radiator surface emissivity of 0.85 and solar absorptivity of 0.2). While this represents a modest penalty for the vertical radiator, it is fully recouped by the availability of two sides for heat rejection resulting in significantly less deployed area. Further, the use of a low-absorptivity, low-emissivity Mylar surface apron can reduce the vertical sink temperature to about 250 K.

## 5.2 Power Conversion

The Power Conversion Module is assumed to begin at the NaK heat exchangers that surround the Stirling heater head; thus the reactor interface would be the pipe stubs on the NaK-to-He heat exchangers. This permits a relatively clean separation point for Reactor Module and BOP flight system development and ATLO. The included power conversion equipment consists of the Stirling power converters and hot-side heat exchangers.

### 5.2.1 Stirling Converter

The reference FSP Stirling converter includes two axially-opposed, free-piston Stirling engines with linear alternators that share a common thermodynamic expansion space. The opposed configuration results in a balanced mechanical system with low vibration to minimize stress on connected fluid joints. The common expansion space assures that the two units operate synchronously for smooth consistent operation. The common expansion space approach may also simplify electrical integration since the units could be operated using a single control circuit. Alternatively, the two engines could be thermodynamically independent, as is the case for the RPS Stirling configuration. However, this approach does not offer any additional fault tolerance unless the individual units include balancing devices to allow their operation without an opposing unit. The FSP system includes four dual-opposed converters to provide redundancy. The use of eight independent units with balancing devices to increase redundancy was deemed an unnecessary complication.

The reference 12 kWe Stirling converter concept is shown in Figure 5-5. The overall length is approximately 1.2 m and the maximum diameter is approximately 0.3 m. The design is based on a scaled-version of the 1 kWe Sunpower EG-1000 (a.k.a. P2A) converter developed for commercial (terrestrial) applications. The engine uses gas bearings and planar springs to assure non-contacting operation of the displacer and piston in the cylinder housing. The internal acceptor and rejector heat exchangers are machined from copper with very small helium flow passages. The regenerator is constructed of random sintered-metal fibers with approximately 90 percent porosity. The total helium volume in the 12 kWe

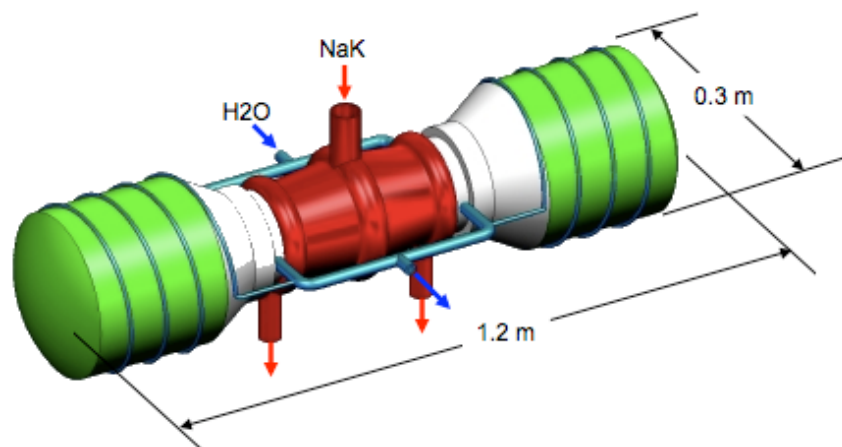


Figure 5-5.—12 kWe dual-opposed Stirling converter.

assembly is 16 liters. The alternator uses samarium-cobalt (SmCo) permanent magnets that allow higher operating temperature and increased radiation resistance compared to the EG-1000's neodymium-iron-boron (NdFeB) magnets. A water-cooling jacket that uses bleed-flow from the main cooling water supply surrounds the alternator vessel to provide temperature control. The Stirling convertors contain various polymers and organics that may be susceptible to radiation damage; thus radiation limits have been set to assure 8 years of operation and testing has begun to verify radiation tolerance. The projected unit flight weight excluding the hot-side heat exchanger and external structure is 72 kg or 6 kg/kWe.

The FSP configuration was designed using the SAGE computer code based on the specified NaK and water fluid interfaces. The design point hot-end temperature is 778 K and the cold-end temperature is 425 K. The original NASA-led SAGE analysis converged on a convertor operating frequency of 75 Hz and a mean helium pressure of 7.5 MPa. Subsequent design optimization performed by Sunpower Inc. under the full-scale Power Conversion Unit (PCU) contract has led to lower frequency (60 Hz) and lower pressure (6.2 MPa).

The piston amplitude in the Sunpower Stirling design is 16 mm for 12 kWe operation. Stirling piston stroke adjustment is the primary method for throttling FSP electric power output; it essentially determines the amount of heat extracted from the NaK. The Stirling power output and alternator voltage are proportional to piston stroke. The expected operating power range of the FSP Stirling convertor is approximately 50 to 110 percent, corresponding to piston amplitudes between 8 and 17.6 mm and alternator output voltages between 200 and 440 Vac rms. The PMAD is designed to maintain the regulated 120 Vdc power bus over this alternator voltage range. The maximum piston stroke is limited by the allowable travel of the piston rod. The minimum stroke is based on sufficient engagement of the gas bearings. FSP system power output could be further reduced by turning-off individual 12 kWe convertors as needed. This provides an effective Stirling power range of 6 kWe (1 convertor at 50 percent power) to about 53 kWe (8 convertors at 110 percent power). However, system operation at this wide range of power output could be constrained by other factors related to the radiator and reactor.

### 5.2.2 Hot-Side Heat Exchanger

The reference NaK heat exchanger has a shared central inlet manifold that splits the NaK flow to each Stirling acceptor. The NaK flows axially in a radial gap across each acceptor and collects at an exit manifold as shown in Figure 5-6. After the exit manifold, the two NaK flow streams are recombined. The original NASA FSP Stirling concept used an Inconel-718 (IN718) heater head. The NaK heat exchanger formed an annular sleeve around the heater head with a 1 mm stainless steel inner wall as an isolation boundary. The IN718 wall thickness was 1.5 mm, and the resulting total temperature drop through the stainless and Inconel was about 31 K. Alternatively, an all-stainless heater head would require a wall thickness of about 9.5 mm to contain the helium pressure and would result in a temperature drop of over 110 K. Given an average NaK temperature at the Stirling of 809 K ( $T_{in} = 824$  K,  $T_{out} = 794$  K), the effective Stirling hot-end temperature is 778 K. The cycle temperature ratio is 778/425 or 1.83, and the estimated fraction of Carnot was 56 percent resulting in a cycle efficiency of about 25 percent.

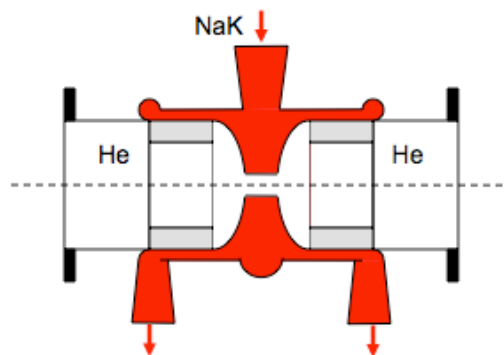


Figure 5-6.—Stirling hot-side heat exchanger concept.

Under the PCU contract, Sunpower has subsequently developed an alternative NaK heat exchanger concept that moves the helium pressure containment outside of the NaK circuit to reduce the heat transfer wall thickness and corresponding temperature drop. The Sunpower PCU design has a slightly improved cycle efficiency of 27 percent as compared to the original NASA concept.

### 5.3 Heat Rejection

The heat rejection module consists of the water heat transport, radiator panels, and deployment mechanisms. FSP heat rejection is somewhat unique relative to other space thermal control systems because of the higher operating temperature and reactor-induced radiation environment. The large radiator size also introduces distinct requirements for stowage and deployment in order to fit within the lander payload envelope. The temperature and radiation requires a careful selection of materials and fluids. The large size combined with the need to be deployable necessitates the use of lightweight materials and modular design strategies.

#### 5.3.1 Heat Transport

The heat transport subsystem is comprised of four pumped water loops, each dedicated to an individual Stirling convertor. Figure 5-7 shows a fluid schematic for one of the two radiator wings that comprise the FSP heat rejection module. A radiator wing includes two water loops servicing two Stirling convertors. Each water loop includes one mechanical pump and volume accumulator. Waste heat is collected at the Stirling convertor and transferred via the pumped water to a radiator manifold. The manifold provides a thermal interface to the evaporator portion of heat pipes that are embedded in the radiator panels. The original NASA concept included evaporators that were bent at approximately 90° relative to the heat pipe condensers to parallel the water manifold. This served to maximize the heat transfer area without introducing bends into the water loop. Heat was transferred from the water to the heat pipe evaporators through a graphite block that was machined to accept the circular tubes. A bumper shield surrounding the manifold was included for micrometeoroid protection.

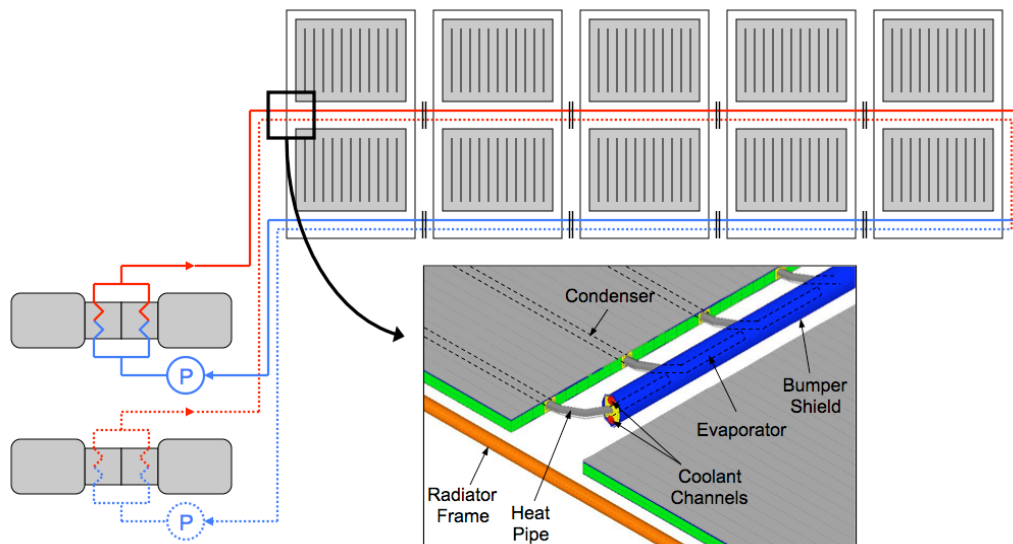


Figure 5-7.—Heat transport schematic.

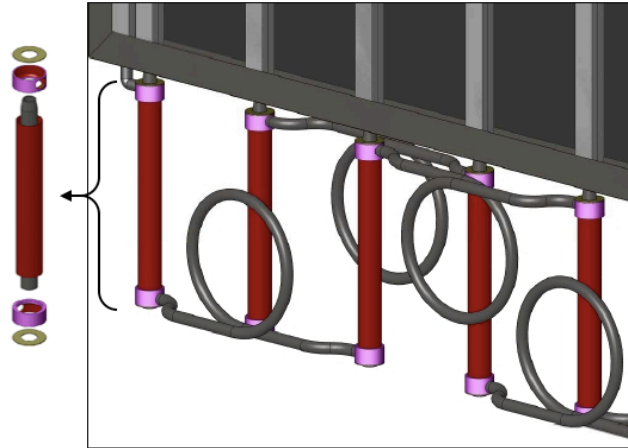


Figure 5-8.—Second generation RDU manifold concept.

This approach resulted in a relatively large temperature drop between the pumped water and the heat pipe. An alternative approach was conceived during the 2nd Generation Radiator Demonstration Unit (RDU) development project as shown in Figure 5-8. Here, the pumped water flows directly over a straight, vertical evaporator section in an annular heat exchanger. This reduces the temperature drop because the heat pipe evaporator is completely immersed in the pumped water flow rather than conductively coupled through a graphite block. The disadvantage is that the water flow circuit is much more complex with an increased number of bends and greater pressure drop. As shown in Figure 5-8, the manifold includes helical interconnects between heat pipes to accommodate thermal expansion/contraction that further increases the pressure drop. The RDU design assumes two separate and independent water flow channels, one for each Stirling heat load, that contact alternating heat pipes. This provides flow loop redundancy while at the same time maximizing available radiator area should one of the loops fail. The alternating heat pipes also provide a possible method to thaw a frozen inactive water circuit using the heated active water flow.

The heat transport subsystem uses 1.6 cm (5/8 in.) diameter titanium plumbing and demineralized water. There are 10 radiator subpanels plumbed in series in a radiator wing and each subpanel has 16 total heat pipes, or 8 per individual water loop. The total heat load per loop including pump heat is 35 kWt. The water enters the radiator wing at 420 K and discharges at 390 K, requiring a water flow rate of about 0.28 kg/s. The total piping length is estimated to be 36 m and the total volume of water is 10.5 liters (2.8 gal) per loop. There are 80 titanium heat pipe heat exchangers per loop with an OD of 2.54 cm surrounding the 1.6 cm (5/8 in.) OD, 25.4 cm (10 in.) long heat pipe evaporators. The total loop pressure drop consists of 80 kPa (12 psi) in piping, 275 kPa (40 psi) in heat pipe heat exchangers, and 30 kPa (4 psi) in the Stirling cold-end heat exchanger. Assuming a 1.2X multiplication factor on the saturation pressure leads to a maximum water loop pressure of about 600 kPa (86 psia). The pump power is 450 W (electric) assuming 25 percent pump efficiency. The mass of the heat transport subsystem including piping, heat exchangers, water coolant, pumps, accumulators, insulation, and heaters for four loops was estimated at about 50 kg per loop.

### 5.3.2 Radiator Assembly

The radiator wings include individual radiator panels with flexible interconnects that can be stowed in an “accordion” arrangement prior to deployment. The radiator panels use a sandwich construction with regularly spaced heat pipes between two polymer-matrix composite facesheets. The circular heat pipes are supported in graphite saddles that provide the thermal interface to the facesheets. The total heat rejected is 70 kWt per wing and the total two-sided radiator area per wing is 92.5 m<sup>2</sup>, including 10 percent area margin. The area margin accounts for degradation of the radiator surface coating that may be attributed to environment effects such as ultraviolet radiation and dust accumulation over the 8 year service life.

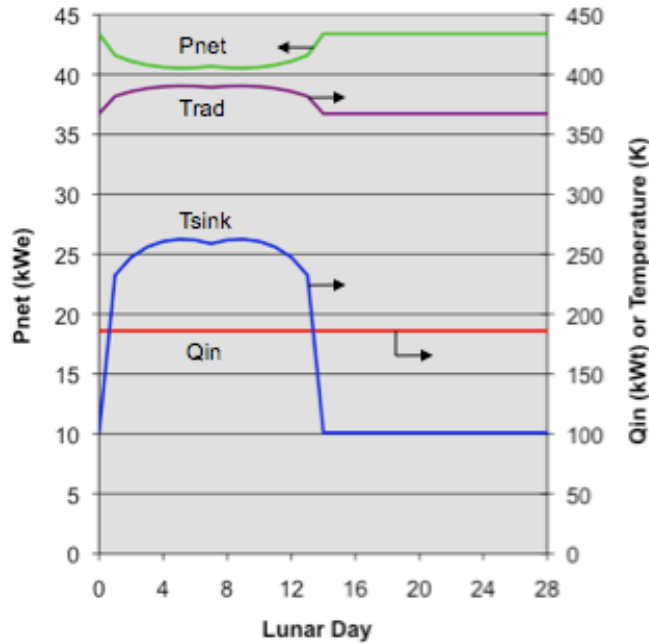


Figure 5-9.—Lunar sink temperature variations and resulting FSP performance.

Radiator sizing is based on worst-case, equatorial Sun angles and includes the contribution of reflected sunlight from the lunar surface on the vertical panels. The use of a Mylar surface apron can reduce the thermal contribution from the surface resulting in a maximum radiator sink temperature of about 250 K. The variation in equatorial sink temperature ( $T_{\text{sink}}$ ) and the corresponding change to the FSP radiator temperature ( $T_{\text{rad}}$ ) and net power ( $P_{\text{net}}$ ) are shown in Figure 5-9 assuming fixed heat input ( $Q_{\text{in}}$ ). The colder sink would permit the system to produce more power during lunar night as a result of the lower power conversion cold-end temperature and higher conversion efficiency. Similarly, the FSP system would produce more power at the lunar poles and Mars due to the lower effective sink temperatures at those locations given the same radiator size.

A radiator wing includes 10 subpanels, measuring approximately 2.7 m wide by 1.7 m tall each. The radiator panel design is also derived from the 2nd Generation RDU development. Each panel includes 16 titanium-water heat pipes. The heat pipes have a 1.27 cm (0.5 in.) OD, 165 cm (65 in.) long condenser section that is encased in a 2.1 cm (0.825 in.) square POCO graphite saddle. A silver-filled thermally-conductive epoxy is used to bond the titanium heat pipes to the POCO and the POCO to the composite facesheets. The facesheets are 0.0635 cm (0.025 in.) thick and consist of multiple layers of K13D2U carbon fibers with Cyanate Ester epoxy resin. The layers are arranged in a matrix that provides high tensile strength and high conductivity (380 W/m-K) in the direction perpendicular to the heat pipes. The current panel design does not include filler material between heat pipes, although that could be added later to meet structural requirements as they are defined. A composite c-channel closeout surrounds the panel edges to improve structural rigidity. The mass of the radiator subpanel including the heat pipes, saddles, facesheets, and close-out channels was estimated at 23 kg. A titanium frame provides the primary structure to support two subpanels as shown in Figure 5-10 as well as a hard-mount interface for the scissor deployment linkages. The radiator assembly would be approximately 3 m wide by 4 m tall. Flexible fluid couplings would be utilized for water transfer between radiator assemblies.

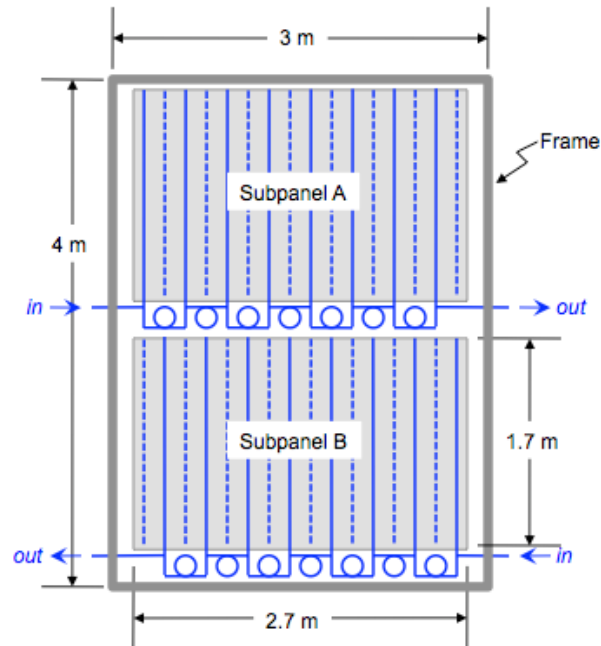


Figure 5-10.—Radiator assembly (1 of 5 per wing).

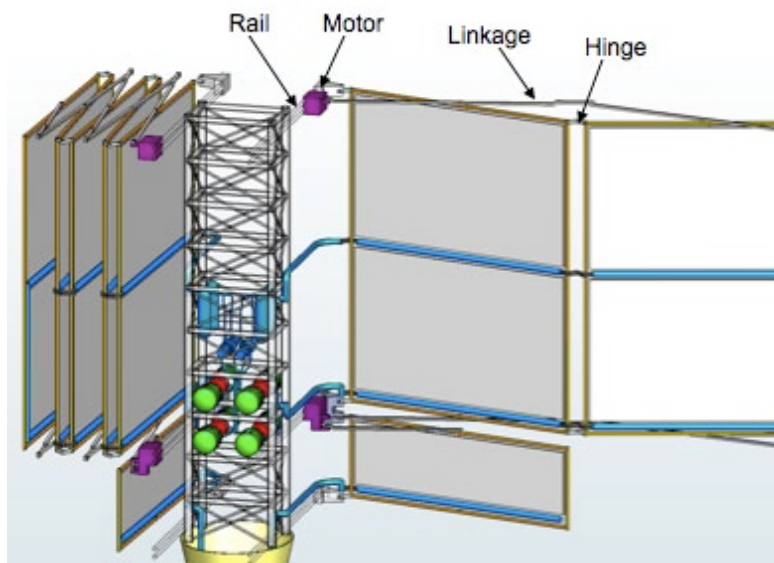


Figure 5-11.—FSP radiator deployment mechanisms.

### 5.3.3 Deployment System

The radiator deployment system is heavily derived from the successful ISS HRS design that uses a motor-driven scissor mechanism (see Fig. 5-3). The radiator assemblies would be mechanically connected via a series of linkages attached at pivot points on the top and bottom of the frame and supplemented with hinges as shown in Figure 5-11. The linkages would be driven by a motor that rides on a set of rails located at the truss. The truss is considered part of the deployment system, although it also serves the purpose of supporting the Stirling converters and reactor I&C components. It is 5 m tall with a 1 by 1.5 m cross-section and is constructed with titanium tubing. The FSP radiators would be designed for remote, autonomous deployment but this could be overridden by manual (crew member) deployment if desired.

## 5.4 Power Management and Distribution

The PMAD module provides the main electrical control functionality for the FSP system. It also provides the interface between the FSP system and the electrical users. In developing the PMAD architecture, effort was given to make the FSP system fully self-sufficient. The PMAD includes all the cabling, controls, diagnostics, and power supplies to operate the system including a solar array and battery for startup power. Further, it provides a regulated 120 Vdc bus interface that allows users to directly connect and disconnect loads. The overall design philosophy is based on parasitic load control meaning that the system generates full power continuously and dissipates any excess power not required by the loads via a resistive load bank. This isolates the thermal power system from electrical transients resulting in fewer thermal cycles and longer service life. The PMAD module consists of the Local Power Controller, Electric Load Interface, Transmission Cabling, and Solar Array/Battery. Most of the equipment would be located remotely from the reactor installation to minimize radiation effects and permit crew maintenance, if required.

### 5.4.1 Local Power Controller

The Local Power Controller (LPC) contains the reactor and power control computers that receive data signals and issue commands to permit autonomous operation of the FSP system. The reactor control computer interprets instrumentation signals and relays commands to power supplies that move control drums or adjust NaK pump flow. Once at steady operation, conditions would be continuously monitored but reactor module adjustments would be fairly infrequent. The power control computer would monitor the Stirling convertors to adjust piston stroke and Parasitic Load Radiator (PLR) setpoint depending on the desired amount of electric power output. In addition, the power control computer would maintain the heat rejection pumps and water loop auxiliary heating, with constant monitoring but fairly infrequent adjustment. The reference system assumes a master and backup computer for both the reactor and power control computers.

The LPC also includes the electronics to convert the Stirling alternator power from ac to dc and regulate the 120 Vdc output for distribution to the Electric Load Interface as shown schematically in Figure 5-12. Each of the eight Stirling alternators has a dedicated power channel that processes the single-phase 60 Hz alternator output. The design-point output voltage is 400 Vac rms at 6 kWe. Stirling output power can be varied between about 50 and 110 percent, corresponding to alternator voltages between 200 and 440 Vac, while maintaining the regulated 120 Vdc bus. The first LPC stage converts the alternator's ac output to 600 Vdc using an active rectifier with power factor control (PFC). This stage delivers a near-constant dc output voltage over a wide range of alternator supply voltages while maintaining optimum power factor. The second stage is a dc-dc converter that converts the 600 to 120 Vdc and provides isolation against electrical faults and grounding issues. Voltage reduction is provided by an inverter and high-frequency transformer-rectifier that can isolate faults. Voltage regulation is performed with a parasitic load controller that senses user load demand and draws any additional current needed to maintain a fixed bus voltage using a resistive load bank. Each pair of Stirling alternators use a separate parasitic load controller. The four parasitic load banks that comprise the PLR are arranged in parallel with the 120 Vdc power bus, separated only by a disconnect switch for each alternator pair.

This PMAD architecture permits the system to produce 120 Vdc regardless of alternator voltage, making partial power operation seamless to the power bus. An additional benefit is that the system can provide regulated power during the FSP startup to expedite the switchover from external power sources.

The LPC electrical components are housed in a 1 by 1 by 1 m aluminum enclosure as shown in Figure 5-13 that includes cold plates and thermal radiators to maintain electronic temperatures below 330 K. The one-sided radiators, providing 2 m<sup>2</sup> surface area, are mounted on the outside of the enclosure and hinged to permit a manual deployment for improved view factor to space. The PLR is sized to dissipate 48 kWe at 770 K. The two-sided PLR, approximately 2 m tall by 1 m wide, would be delivered separately and attached to the top of LPC at the outpost.

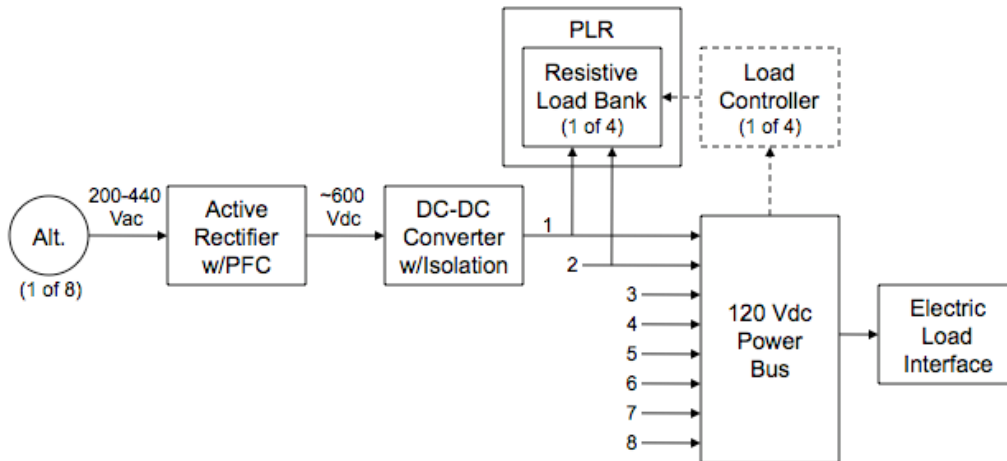
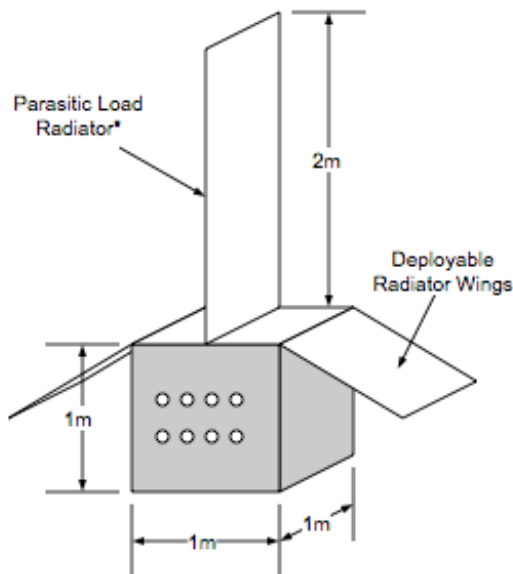


Figure 5-12.—PMAD electrical schematic.



\*Attached by crew or robot after delivery to lunar surface.

Figure 5-13.—LPC enclosure and radiators.

### 5.4.2 Electric Load Interface

1 The Electric Load Interface (ELI) serves as the FSP system’s interface to the outpost. It provides the access point for FSP-generated electric power and the communications link for FSP system operations data. There are two separate power distribution nodes, one for outpost user loads and the other for FSP auxiliary loads. The user load interface is envisioned as an electrical switch panel, similar to a residential breaker box, which would allow users to connect various size loads as required. The auxiliary power panel would feed individual power supplies located with the ELI that provide the electrical input for FSP pumps, motors, heaters, and sensors. A system interface computer provides supervisory control for the ELI functions. The ELI components are housed in a second 1 by 1 by 1 m aluminum enclosure with external radiators, similar to the LPC shown in Figure 5-13 but without the PLR.

### 5.4.3 Transmission Cabling

The transmission cabling for the reference (buried) FSP system includes the main power cable from the Stirling alternators to the LPC, the data cabling from the truss-mounted instrumentation relays to the

LPC, and the auxiliary power cable from the ELI back to the reactor installation. All cabling is assumed to be placed on the surface with a 180° view to space. It would be delivered to the lunar surface in a cable spool and deployed using either a telerobotic rover or crew members. The cabling is based on space-proven MIL-STD ETFE (ethylene-tetrafluoroethylene) insulated, tin-coated copper conductor rated for up to 600 V and 150 °C. All cables are 125 m long which includes 25 percent length margin relative to the 100 m separation distance. The eight 6 kWe, 400 Vac alternator power cables carry about 9.1 A each and require two 14 AWG conductors. Total resistance is 1.25 Ω resulting in about 200 W power loss, which is equivalent to 96 percent transmission efficiency. The data cabling is assumed to include four 16 AWG conductors, two primary and two backup. The auxiliary power cabling is assumed to include twenty 10 AWG conductors suitable for up to ten 500 W power loads at 120 Vdc, or 5 kWe total. Total resistance is 0.52 Ω resulting in about 18 W power loss per 500 W cable. The auxiliary power cables would be grouped as necessary to meet the various FSP parasitic loads at the reactor installation.

#### 5.4.4 Solar Array and Battery

A 5 kWe photovoltaic (PV) solar array and three 10 kW-hr batteries are included with the FSP PMAD module and connected to the 120 Vdc ELI at the outpost. The solar array is assumed to be a derivative of the 5.5 m diameter ATK UltraFlex array being developed for the Orion Crew Exploration Vehicle. It is designed for compact stowage and simple deployment to form a circular Sun-tracking PV surface. The batteries utilize Li-ion cells and are identical to battery modules planned for Orion. By the time that these items are needed for FSP, they will be fully proven with the Orion vehicle. It may also be possible to start the FSP system without solar arrays depending on the mission timeline and environment.

The available power provided by the Solar Array and Battery subsystem is sufficient for starting the FSP system during daylight or maintaining a non-operating FSP system during a 354 hr lunar night. It would also be available should there ever be a need to power-down the FSP system. A notional FSP startup power profile is shown in Figure 5-14. Startup would be performed over a period of approximately one Earth-day with pauses at incremental steps during the ascent to full power. The first 5 to 6 hr (shown in the inset of Fig. 5-14) would be the most power intensive and would include radiator panel deployment, water loop charging, NaK and water fluid pumping, and Stirling electrical motoring. Maximum power draw is almost 5 kWe between hours 4 and 5. At the 8-hr mark, the system is at “break-even” power. By the 10-hr mark, the system is producing 25 percent power and is no longer dependent on the solar array and battery. By the 18-hr mark, the system is at full power providing 45 kWe at the PMAD power bus (48 kWe from the Stirling units) with up to 5 kWe available for the auxiliary FSP loads. It should be noted that this process could be extended, if desired, to gather additional reactivity data for the purpose of fully characterizing reactor performance before beginning full power operations.

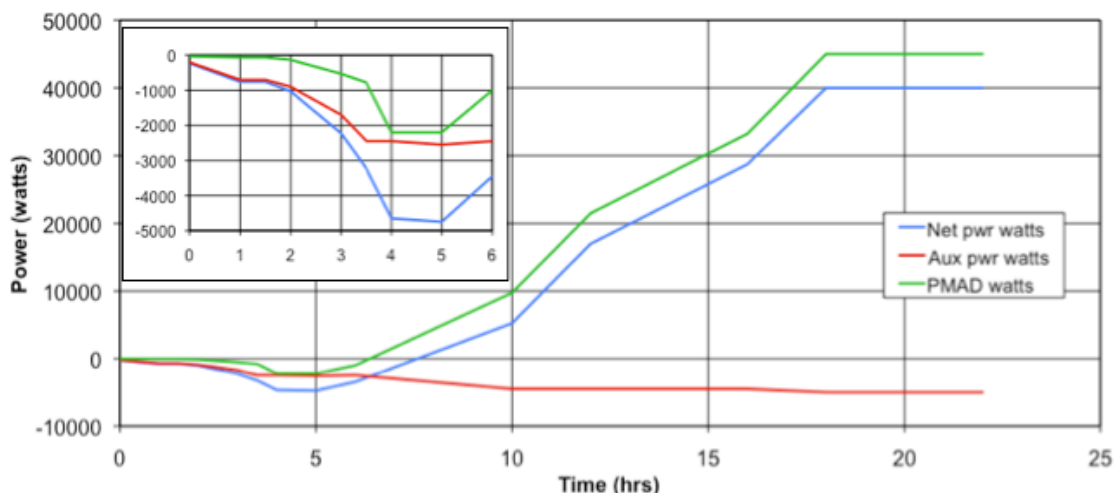


Figure 5-14.—Estimated FSP startup profile.

## 6.0 Conclusions

This document provides a summary of design efforts performed by the FSP team between January 2008 and June 2009. Prior to 2008, the NASA/DOE team completed the Affordable Fission Surface Power System Study and selected a Preliminary FSP Reference Concept. The FSP capability was explored through a series of NASA architecture studies where various mission integration options were evaluated. The results indicated that FSP technology could offer significant mission benefits. The FSP team proceeded to investigate the design details of the concept through trade studies and analysis. Many design decisions were made related to the Reactor Module and Balance-of-Plant. The results, reported herein, provide a foundation for future studies. The FSP technology project plans to conduct extensive hardware testing and use the results to improve analytical models that can be applied to refine this design concept. The end goal is hardware-based FSP design concept that can serve as a starting point for an FSP flight development program.



## Appendix—Fission Surface Power System Master Equipment List

FSPS off-loaded and buried in 2.3m hole at 100m separation		Materials	Quantity	Unit (kg)	CBE (kg)	Margin	Total (kg)	Comments
<b>6.0</b>	<b>Fission Surface Power System</b>				<b>5819.9</b>	<b>19%</b>	<b>6941.8</b>	<b>40 kWe net</b>
<b>6.1</b>	<b>Reactor Module</b>				<b>1440.3</b>	<b>30%</b>	<b>1872.4</b>	
6.1.1	Reactor Core Subsystem				144.3			186 kWt
6.1.1.1	Fuel Pin	UO2/SS	163	0.7	112.5			860K max clad
6.1.1.2	Core Internal Structure	SS	1	2.1	2.1			
6.1.1.3	Core Coolant	NaK	1	5.1	5.1			
6.1.1.4	Core Vessel	SS	1	24.6	24.6			
6.1.2	Reflector Subsystem				295.0			
6.1.2.1	Fixed Radial Reflector	Be/SS	1	119.5	119.5			
6.1.2.2	Rotating Drum Reflector	Be/B4C/SS	6	22.6	135.6			
6.1.2.3	Reactor Insulation	MFI	1	0.0	0.0			
6.1.2.4	Reactor External Structure	SS	1	39.9	39.9			
6.1.3	Primary Heat Transport Subsystem				422.0			850K core exit, 50K dT
6.1.3.1	Primary Loop Piping	SS	1	17.7	17.7			
6.1.3.2	Primary Pump	SS	2	135.1	270.3			4.3 kg/s, 0.8 kWe
6.1.3.3	Primary Accumulator	SS	1	7.5	7.5			
6.1.3.4	Primary Loop Coolant	NaK	1	45.7	45.7			
6.1.3.5	Primary Loop Insulation	MFI	1	5.2	5.2			
6.1.3.6	Primary Loop Heater		1	31.7	31.7			
6.1.3.7	Primary Loop Structure	SS	1	43.8	43.8			
6.1.4	Intermediate Heat Transport Subsystem				386.0			824K IHX exit, 30K dT
6.1.4.1	Intermediate Heat Exchanger	SS	2	26.3	52.6			
6.1.4.2	Intermediate Loop Piping		2	6.3	12.7			
6.1.4.3	Intermediate Pump	SS	2	89.4	178.7			3.5 kg/s, 0.3 kWe x2
6.1.4.4	Intermediate Accumulator	SS	2	5.0	10.0			
6.1.4.5	Intermediate Loop Coolant	NaK	2	27.9	55.9			
6.1.4.6	Intermediate Loop Insulation	MFI	2	2.2	4.4			
6.1.4.7	Intermediate Loop Heater		2	15.9	31.7			
6.1.4.8	Intermediate Loop Structure	SS	2	20.0	40.0			
6.1.5	Instrumentation and Control Subsystem				98.0			5Mrad, 1x10 <sup>14</sup> nvt
6.1.5.1	Reflector Drive Motors		6	4.0	24.0			
6.1.5.2	Gear Box Assembly		6	2.0	12.0			
6.1.5.3	Motor Drive Electronics		2	2.5	5.0			
6.1.5.4	Sensor Electronics		2	2.5	5.0			
6.1.5.5	Reactor Sensors		1	2.0	2.0			
6.1.5.6	Primary Loop Sensors		1	2.0	2.0			
6.1.5.7	Intermediate Loop Sensors		2	2.0	4.0			
6.1.5.8	Power Conversion Sensors		4	2.0	8.0			
6.1.5.9	Heat Rejection Sensors		4	2.0	8.0			
6.1.5.10	I&C Enclosure	Al	4	2.0	8.0			
6.1.5.11	I&C Spot Shielding	Pb	4	5.0	20.0			
6.1.6	Reactor Cavity Cooling Subsystem	SS/H2O	1	95.0	95.0			400K
<b>6.2</b>	<b>Power Conversion Module</b>				<b>411.2</b>	<b>30%</b>	<b>534.6</b>	
6.2.1	Hot-end Heat Exchanger Subsystem	SS	4	10.0	40.0			
6.2.2	Power Generation Subsystem				371.2			
6.2.2.1	Stirling Convertor	IN/SS	4	72.0	288.0			12 kWe each, Th=778K, Tc=425K
6.2.2.2	Vessel Cooling Jacket	SS	8	5.0	40.0			
6.2.2.3	Power Conversion Insulation	MFI	4	3.6	14.4			
6.2.2.4	Power Conversion Structure	SS	4	7.2	28.8			
<b>6.3</b>	<b>Heat Rejection Module</b>				<b>766.5</b>	<b>30%</b>	<b>996.5</b>	
6.3.1	Secondary Heat Transport Subsystem				203.9			
6.3.1.1	Secondary Piping	Ti	4	6.7	26.8			390K radiator exit, 30K dT
6.3.1.2	Heat Pipe Heat Exchangers	Ti	320	0.1	25.0			
6.3.1.3	Secondary Pump	Ti	4	19.0	75.8			0.3 kg/s, 0.5 kWe x4
6.3.1.4	Secondary Accumulator	Ti	4	4.2	16.7			
6.3.1.5	Secondary Loop Coolant	H2O	4	9.8	39.0			
6.3.1.6	Secondary Loop Insulation	MFI	4	4.2	16.7			
6.3.1.7	Secondary Loop Heater		4	1.0	4.0			
6.3.2	Radiator Subsystem				510.0			2 wings, 70 kWt per wing
6.3.2.1	Radiator Panel	Ti/H2O/PMC	20	23.0	460.0			2.7x1.7m each, 20mm thick
6.3.2.2	Radiator Frame	Ti	10	5.0	50.0			
6.3.2.3	Surface Apron	Mylar	2	0.0	0.0			
6.3.3	Deployment Subsystem				52.6			
6.3.3.1	Support Truss	Ti	1	25.0	25.0			5m tall
6.3.3.2	Radiator Drive Motor		4	2.0	8.0			
6.3.3.3	Deployment Rail	Ti	4	2.0	8.0			
6.3.3.4	Deployment Linkage	Ti	20	0.5	10.0			
6.3.3.5	Deployment Hinges	Ti	16	0.1	1.6			

FSPS off-loaded and buried in 2.3m hole at 100m separation		Materials	Quantity	Unit (kg)	CBE (kg)	Margin	Total (kg)	Comments
<b>6.4</b>	<b>Power Management and Distribution Module</b>				<b>1070.7</b>	<b>30%</b>	<b>1391.9</b>	
6.4.1	Local Power Controller Subsystem				278.2			Located at outpost
6.4.1.1	Reactor Control Computer		2	5.0	10.0			
6.4.1.2	Power Control Computer		2	5.0	10.0			
6.4.1.3	LPC Electronics		8	24.0	192.0			8x6 kWe, 400Vac to 120Vdc
6.4.1.4	Parasitic Load Radiator		1	40.0	40.0			48 kWe+20%, 770K, 4m2
6.4.1.5	LPC Enclosure	Al	1	16.2	16.2			1x1x1m box, 1mm thick
6.4.1.6	LPC Thermal Control	Al	1	10.0	10.0			330K, 2m2
6.4.2	Transmission Cabling Subsystem				180.0			
6.4.2.1	Main Power Cabling	ETFE	8	6.0	48.0			8x6 kWe, 400 Vac, 100m+25%
6.4.2.2	High Voltage Cabling	Kapton/Al	8	0.0	0.0			
6.4.2.3	Data Cabling	ETFE	2	6.0	12.0			100m+25%
6.4.2.4	Auxiliary Power Cabling	ETFE	10	12.0	120.0			10x0.5 kWe, 120Vdc, 100m+25%
6.4.3	Electrical Load Interface Subsystem				157.5			Located at outpost
6.4.3.1	System Interface Computer		2	5.0	10.0			
6.4.3.2	User Load Bus		1	5.0	5.0			120Vdc
6.4.3.3	Auxiliary Load Bus		1	5.0	5.0			120Vdc
6.4.3.4	Primary Pump Power Supply		2	16.1	32.2			
6.4.3.5	Intermediate Pump Power Supply		2	16.1	32.2			
6.4.3.6	Secondary Pump Power Supply		4	2.0	8.0			
6.4.3.7	Reflector Drive Power Supply		6	1.0	6.0			
6.4.3.8	Radiator Drive Power Supply		4	1.0	4.0			
6.4.3.9	Primary Loop Heater Power Supply		1	2.0	2.0			
6.4.3.10	Intermediate Loop Heater Power Supply		2	2.0	4.0			
6.4.3.11	Secondary Loop Heater Power Supply		4	2.0	8.0			
6.4.3.12	Communications Link		1	10.0	10.0			
6.4.3.13	ELI Enclosure	Al	1	16.2	16.2			1x1x1m box, 1mm thick
6.4.3.14	ELI Thermal Control	Al	1	15.0	15.0			330K, 3m2
6.4.4	Solar Array Battery Subsystem				455.0			
6.4.4.1	Solar Array	GaAs	1	110.0	110.0			1x5 kW Orion array
6.4.4.2	Battery	Li	3	66.7	200.0			3x10 kWh batteries, 150 Whr/kg
6.4.4.3	Avionics		1	36.5	36.5			
6.4.4.4	Main Bus Switching Unit		1	80.0	80.0			
6.4.4.5	Cabling		1	15.0	15.0			
6.4.4.6	Structure		1	10.0	10.0			
6.4.4.7	Command & Data Handling		1	3.5	3.5			
6.4.5	Remote Power Controller Subsystem				0.0			
6.4.5.1	RPC Computer		1	0.0	0.0			
6.4.5.2	RPC Electronics		1	0.0	0.0			
6.4.5.3	RPC Enclosure	Al	1	0.0	0.0			
6.4.5.4	RPC Thermal Control	Al	1	0.0	0.0			
<b>6.5</b>	<b>Radiation Shield Module</b>				<b>2080.0</b>	<b>0%</b>	<b>2080.0</b>	
6.5.1	Integral Neutron Shield Subsystem		1		2030.0			3 mrem/hr at 100m
6.5.1.1	Neutron Shield	B4C	1	1940.0	1940.0			
6.5.1.2	Neutron Shield Structure	SS	1	90.0	90.0			
6.5.2	Integral Gamma Shield Subsystem	DU	0	0.0	0.0			
6.5.3	External Shroud Subsystem	SS	1	50.0	50.0			
<b>6.6</b>	<b>Integration Structure</b>				<b>51.1</b>	<b>30%</b>	<b>66.5</b>	
6.6.1	Lander Integration Structure	SS	1	42.8	42.8			
6.6.2	Regolith Containment Subsystem	Al	0	0.0	0.0			
6.6.3	Handling Integration Structure	SS	1	3.6	3.6			
6.6.4	Installation Integration Structure	SS	1	4.7	4.7			

## References

1. *Affordable Fission Surface Power System Study Final Report*, Exploration Systems Mission Directorate Memorandum for the Record, 5 October 2007.
2. *Executive Summary of Reference Fission Surface Power System Concept Selection*, Exploration Systems Mission Directorate Memorandum for the Record, 23 July 2008.
3. Lee Mason, David Poston, and Louis Qualls, “System Concepts for Affordable Fission Surface Power,” NASA/TM—2008-215166, January 2008.
4. *Human Exploration of Mars: Design Reference Architecture 5.0*, Bret G. Drake, editor, NASA/SP—2009-566, July 2009.
5. David I. Poston, Lee S. Mason, and Michael G. Houts, “Radiation Shielding Architecture Studies for NASA’s Lunar Fission Surface Power System,” *Proceedings of Nuclear and Emerging Technologies for Space (NETS-2009)*, Atlanta GA, 14–19 June 2009, Paper 208590.

REPORT DOCUMENTATION PAGE			Form Approved OMB No. 0704-0188		
<p>The public reporting burden for this collection of information is estimated to average 1 hour per response, including the time for reviewing instructions, searching existing data sources, gathering and maintaining the data needed, and completing and reviewing the collection of information. Send comments regarding this burden estimate or any other aspect of this collection of information, including suggestions for reducing this burden, to Department of Defense, Washington Headquarters Services, Directorate for Information Operations and Reports (0704-0188), 1215 Jefferson Davis Highway, Suite 1204, Arlington, VA 22202-4302. Respondents should be aware that notwithstanding any other provision of law, no person shall be subject to any penalty for failing to comply with a collection of information if it does not display a currently valid OMB control number.</p> <p>PLEASE DO NOT RETURN YOUR FORM TO THE ABOVE ADDRESS.</p>					
<b>1. REPORT DATE (DD-MM-YYYY)</b> 01-08-2010		<b>2. REPORT TYPE</b> Technical Memorandum		<b>3. DATES COVERED (From - To)</b>	
<b>4. TITLE AND SUBTITLE</b> Fission Surface Power System Initial Concept Definition			<b>5a. CONTRACT NUMBER</b>		
			<b>5b. GRANT NUMBER</b>		
			<b>5c. PROGRAM ELEMENT NUMBER</b>		
<b>6. AUTHOR(S)</b> Fission Surface Power, Team			<b>5d. PROJECT NUMBER</b>		
			<b>5e. TASK NUMBER</b>		
			<b>5f. WORK UNIT NUMBER</b> WBS 463169.02.03.01.01		
<b>7. PERFORMING ORGANIZATION NAME(S) AND ADDRESS(ES)</b> National Aeronautics and Space Administration John H. Glenn Research Center at Lewis Field Cleveland, Ohio 44135-3191			<b>8. PERFORMING ORGANIZATION REPORT NUMBER</b> E-17359		
<b>9. SPONSORING/MONITORING AGENCY NAME(S) AND ADDRESS(ES)</b> National Aeronautics and Space Administration Washington, DC 20546-0001			<b>10. SPONSORING/MONITOR'S ACRONYM(S)</b> NASA		
			<b>11. SPONSORING/MONITORING REPORT NUMBER</b> NASA/TM-2010-216772		
<b>12. DISTRIBUTION/AVAILABILITY STATEMENT</b> Unclassified-Unlimited Subject Category: 20 Available electronically at <a href="http://gltrs.grc.nasa.gov">http://gltrs.grc.nasa.gov</a> This publication is available from the NASA Center for AeroSpace Information, 443-757-5802					
<b>13. SUPPLEMENTARY NOTES</b>					
<b>14. ABSTRACT</b> Under the NASA Exploration Technology Development Program (ETDP) and in partnership with the Department of Energy (DOE), NASA has embarked on a project to develop Fission Surface Power (FSP) technology. The primary goals of the project are to 1) develop FSP concepts that meet expected surface power requirements at reasonable cost with added benefits over other options, 2) establish a hardware-based technical foundation for FSP design concepts and reduce overall development risk, 3) reduce the cost uncertainties for FSP and establish greater credibility for flight system cost estimates, and 4) generate the key products to allow NASA decision-makers to consider FSP as a preferred option for flight development. The FSP project was initiated in 2006 as the Prometheus Program and the Jupiter Icy Moons Orbiter (JIMO) mission were phased-out. As a first step, NASA Headquarters commissioned the Affordable Fission Surface Power System Study to evaluate the potential for an affordable FSP development approach. With a cost-effective FSP strategy identified, the FSP team evaluated design options and selected a Preliminary Reference Concept to guide technology development. Since then, the FSP Preliminary Reference Concept has served as a point-of-departure for several NASA mission architecture studies examining the use of nuclear power and has provided the foundation for a series of "Pathfinder" hardware tests. The long-term technology goal is a Technology Demonstration Unit (TDU) integrated system test using full-scale components and a non-nuclear reactor simulator. The FSP team consists of Glenn Research Center (GRC), Marshall Space Flight Center (MSFC) and the DOE National Laboratories at Los Alamos (LANL), Idaho (INL), Oak Ridge (ORNL), and Sandia (SNL). The project is organized into two main elements: Concept Definition and Risk Reduction. Under Concept Definition, the team performs trade studies, develops analytical tools, and formulates system concepts. Under Risk Reduction the team develops hardware prototypes and conducts laboratory-based testing.					
<b>15. SUBJECT TERMS</b> Nuclear electric power generation					
<b>16. SECURITY CLASSIFICATION OF:</b>			<b>17. LIMITATION OF ABSTRACT</b>  UU	<b>18. NUMBER OF PAGES</b>  58	
<b>a. REPORT</b> U	<b>b. ABSTRACT</b> U	<b>c. THIS PAGE</b> U			<b>19a. NAME OF RESPONSIBLE PERSON</b> STI Help Desk (email: <a href="mailto:help@sti.nasa.gov">help@sti.nasa.gov</a> )
			<b>19b. TELEPHONE NUMBER (include area code)</b> 443-757-5802		



